HHS Public Access

Author manuscript

ACS Biomater Sci Eng. Author manuscript; available in PMC 2022 September 13.

Published in final edited form as:

ACS Biomater Sci Eng. 2021 September 13; 7(9): 4027–4047. doi:10.1021/acsbiomaterials.0c01547.

Detecting and Monitoring Hydrogels with Medical Imaging

Yuxi C. Dong,
Department of Radiology and Department of Bioengineering, University of Pennsylvania, Philadelphia, Pennsylvania 19104, United States

Mathilde Bouché
Université de Lorraine, CNRS, L2CM UMR 7053, F-54000 Nancy, France

Selen Uman, **Jason A. Burdick**
Department of Bioengineering, University of Pennsylvania, Philadelphia, Pennsylvania 19104, United States

David P. Cormode
Department of Radiology and Department of Bioengineering, University of Pennsylvania, Philadelphia, Pennsylvania 19104, United States

Abstract

Hydrogels, water-swollen polymer networks, are being applied to numerous biomedical applications, such as drug delivery and tissue engineering, due to their potential tunable rheologic properties, injectability into tissues, and encapsulation and release of therapeutics. Despite their promise, it is challenging to assess their properties *in vivo* and crucial information such as hydrogel retention at the site of administration and *in situ* degradation kinetics are often lacking. To address this, technologies to evaluate and track hydrogels *in vivo* with various imaging techniques have been developed in recent years, including hydrogels functionalized with contrast generating material that can be imaged with methods such as X-ray computed tomography (CT), magnetic resonance imaging (MRI), optical imaging, and nuclear imaging systems. In this review, we will discuss emerging approaches to label hydrogels for imaging, review the advantages and limitations of these imaging techniques, and highlight examples where such techniques have been implemented in biomedical applications.

Graphical Abstract

Corresponding Author: **David P. Cormode** – Department of Radiology and Department of Bioengineering, University of Pennsylvania, Philadelphia, Pennsylvania 19104, United States; Phone: 215-615-4656; David.Cormode@pennmedicine.upenn.edu; Fax: 240-368-8096.

Complete contact information is available at: https://pubs.acs.org/10.1021/acsbiomaterials.0c01547

The authors declare no competing financial interest.

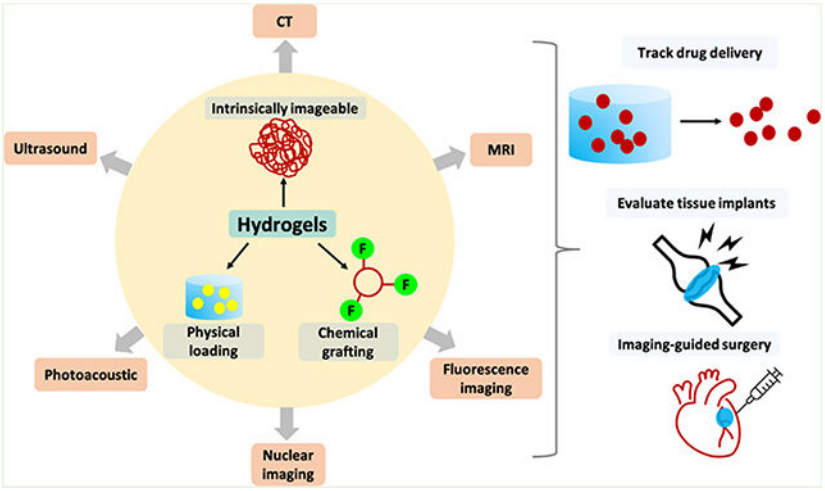

Keywords

hydrogels; biomedical imaging; contrast agents; magnetic resonance imaging; computed tomography; fluorescence imaging

1. INTRODUCTION

Hydrogels are solid materials mainly constituted of water, composed of a three-dimensional cross-linked polymer or colloidal network immersed in fluids, and they have found utility across many fields.[1,2] In the past decades, hydrogels have become increasingly important in diverse biomedical applications, such as drug delivery and tissue engineering, due to their unique characteristics, such as high water content, tunable properties, controllable degradation, and their potential responsiveness to extrinsic signals.[3–5] Hydrogels are fabricated by numerous polymerization and cross-linking strategies to form polymeric networks[6] and are generally classified into two categories based on the nature of their cross-linking, namely, physically or chemically cross-linked hydrogels.[7,8] Of these, physically cross-linked hydrogels are assembled through noncovalent cross-linking (e.g., ionic interactions, hydrogen bonding),[6,9] whereas chemically cross-linked hydrogels involve covalent bonds within their cross-links.[10,11] The cross-links can be designed to be reversible so the hydrogels possess shear-thinning properties, which can be advantageous in biomedical applications.[12,13]

Owing to these unique characteristics, hydrogels can be designed for minimally invasive delivery to a tissue site of interest, where accurate localization and monitoring of the hydrogel are of great importance.[3,14,15] Meanwhile, the *in vivo* degradation of hydrogels can play an important role in achieving desired therapeutic outcomes.[16] Thus, the ability to image hydrogels is useful to confirm that the hydrogel has been successfully administered to the target site and in the correct quantity as well as to monitor the hydrogel erosion over time. In many instances, groups of animals are sacrificed either soon after injection or at staggered time points, and the residual hydrogel is removed for examination in order to monitor the state of implanted hydrogels *in vivo*.[17,18] Thus,

serial postadministration imaging of hydrogels would yield improved information on hydrogel placement, degradation *in vivo*, or the release of therapeutics, due to the need for fewer animals and to allow comparisons across the same animal. To accomplish this, hydrogels can be rendered imageable with various medical imaging modalities by using intrinsically imageable polymers during hydrogel formation or by functionalizing hydrogels with contrast-generating materials through physical loading or chemical grafting.[1,15,19,20]

To date, multiple imaging modalities and their combinations have been used for different clinical applications[21–30] as well as used for detecting and monitoring hydrogels in tissues, with each of them having their own advantages and limitations (Tables 1 and 2).[31–39] For example, CT is one of the most widely used clinical imaging modalities, where computerized X-ray imaging is used to produce three-dimensional, anatomic images with high spatial and temporal resolution.[40] To distinguish hydrogels from the surrounding soft tissues in CT, X-ray contrast agents are usually used. The currently approved contrast agents for X-ray imaging are iodinated small molecules or barium sulfate suspensions. Although both can be incorporated into the hydrogel to impart radiopacity, they can cause adverse events and have shortcomings in their specificity of detection.[41,42] With the same capability of rendering hydrogels radiopaque, nanoparticle-based contrast agents such as gold nanoparticles (AuNP) can produce more contrast than iodinated contrast agents, and their versatility also allows for a wider range of applications. While other X-ray based imaging modalities such as conventional radiography, spectral photon-counting computed tomography (SPCCT), mammography, and fluoroscopy would offer similar benefits to utilizing radiopaque hydrogels, there have been only a few studies reporting the use of these modalities for hydrogel imaging as compared to more commonly used CT.[43–45]

As another example of an imaging modality, MRI uses a large magnetic field and radio waves to perform anatomical imaging of soft tissues.[46] It is a noninvasive and nondestructive diagnostic tool with good potential for monitoring tissue implants.[47,48] Similar to CT, MRI uses contrast agents to enhance internal structures. Gadolinium chelates are the only type of MRI contrast agents both approved by the FDA and available on the market.[49,50] Superparamagnetic iron oxide nanoparticles have been FDA-approved as MRI contrast agents; however, all have been withdrawn from the market due to low sales.[51] The one remaining iron oxide nanoparticle on the market, ferumoxytol, is approved for iron replacement therapy, so its applications as an MRI contrast agent are off-label uses. Hydrogels can either be functionalized with contrast agents such as these so that they can be distinguished from adjacent tissues with conventional MRI or certain types of hydrogel can be induced to produce contrast in the absence of exogenous contrast agents via techniques such as chemical exchange saturation transfer (CEST) MRI.[32,52,53]

Fluorescence imaging relies on the absorption and scattering properties of light in tissue or biomaterial components.[54,55] Its high sensitivity, resolution, and high throughput render this technique popular for *in vivo* imaging.[56] However, its low tissue penetration (<1 cm) and limited quantitative accuracy limits its utility. Probes that absorb in the near-infrared (NIR) region(i.e., 650–900 nm) are often used for *in vivo* imaging as most tissues have relatively low absorbance in the NIR region.[57] Thus, noninvasive *in vivo* tracking of the distribution and degradation of hydrogels can be achieved by labeling the hydrogel with fluorescent

probes such as fluorophores (indocyanine green and methylene blue are the only two NIR fluorophores approved by FDA), quantum dots, or upconversion nanoparticles.[58–62] In addition to these techniques, other imaging modalities such as nuclear imaging, ultrasound, and photoacoustic imaging can also be used to visualize the *in vivo* distribution and degradation of hydrogels, although these modalities remain relatively underexplored for these applications.[36,63,64]

In the following sections, we first summarize the various strategies used in the cross-linking of hydrogels, which is important to inform hydrogel properties and subsequent imaging approaches. Next, the approaches that have been taken for the functionalization of hydrogels to render them imageable are reviewed. We then focus on recent developments in the imaging of hydrogels using modalities such as CT, MRI, and fluorescence imaging. For each imaging modality, the basic principles of the imaging method are first described, and then the biomedical applications using the technique are reviewed. Lastly, the potential and challenges of hydrogel imaging in clinical settings are addressed.

2. OVERVIEW OF HYDROGEL FUNDAMENTALS

Hydrogels can be classified based on the polymer source (natural, synthetic), polymer composition (homopolymer, copolymer, interpenetrating, nanocomposite), polymer configuration (amorphous, semicrystalline, crystalline), network degradability (biodegradable, nondegradable), and type of cross-linking.[4] These variables give rise to hydrogels with a wide range of biochemical and biophysical properties that can be tailored for specific applications.

Natural polymers such as polysaccharides (e.g., hyaluronic acid (HA), chitosan, heparin) and proteins (e.g., gelatin) are derived from natural sources and often inherently incorporate important functional features, such as being biocompatible, biodegradable, and presenting critical biological cues. These natural polymers can be modified with various functional groups for cross-linking into networks for hydrogel formation. Synthetic polymers such as polypeptides, polyesters, polyanhydrides, and polyphosphazenes can be designed with specific features in mind, such as tunable degradation rates, mechanical properties, and microstructures.[65] Furthermore, they are designed to incorporate functional groups during synthesis to allow for cross-linking. Nondegradable synthetic hydrogels have been prepared from the copolymerization of various vinylated monomers or macromers such as 2-hydroxyethyl methacrylate (HEMA), acrylamide (AAm), acrylic acid (AAc), *N*-isopropylacrylamide (NIPAm), and polyethylene glycol (PEG).[66] For example, the end hydroxyl groups of PEG can be modified with functional groups (e.g., thiols, acrylates), allowing many different cross-linking methods to form hydrogels.[67] Similarly, poly(vinyl alcohol) (PVA) is another common synthetic polymer with pendant hydroxyl groups that can be modified for cross-linking with different chemical methods[68] as well as with freeze/thaw cycles to induce physical cross-linking.[69]

Chemically cross-linked networks traditionally have permanent cross-linking points or junctions, while physical networks have reversible junctions that are formed through polymer chain entanglements or physical interactions (e.g., ionic interactions, metal

coordination, hydrogen bonds). Recently, dynamic covalent networks have also emerged as a means to chemically cross-link hydrogels, whereby bond cleavage can occur under mechanical shear and reform to exhibit self-healing properties. In this section, we review the common methods of physical and chemical cross-linking to form imageable hydrogels.

2.1. Physical Cross-Linking.

Physical associations that are used to form hydrogels from polymer chains include ionic interactions,[70] metal–ligand coordination,[71] hydrogen bonding,[72] hydrophobicity,[73] and supramolecular host–guest[74] interactions. The self-assembly of physically cross-linked hydrogels enables rapid hydrogel formation while avoiding the use of any external cross-linking agents. These physical associations are reversible and contribute to the shear-thinning and self-healing properties of many hydrogels, which allows injectability and processing using techniques such as 3D printing. These features are reviewed extensively elsewhere.[75]

One of the simplest approaches to hydrogel formation is the ionic cross-linking of charged biopolymers with multivalent ions. For example, alginate is a naturally occurring, anionic, and hydrophilic polymer that cross-links in the presence of cations, most typically Ca^{2+}, and is commonly used for tissue engineering and drug delivery applications. Recently, radionuclides such as In^{3+} and Zr^{4+} were used to cross-link alginate, providing a novel and simple hydrogel radiolabeling approach.[63] Hydrogen bonding, represented as an attractive interaction between hydrogen atoms and electronegative atoms such as nitrogen, oxygen, and fluorine, has also been used in hydrogel formation. For example, many binding motifs such as ureiodopyrimidone (UPy),[76] benzene-1,3,5 tricarboxamide,[77] and catechols[78] have been used to functionalize polymers for the formation of hydrogels through hydrogen bonding. Recently, PEG end-functionalized with UPy moieties as well as DOTA-Gd(III) were used to form fibrous hydrogels based on pH that could be visualized via MRI after injection into the myocardium.[48]

Metal–ligand coordination complexes offer near-covalent stabilities with pH-tunable kinetics and have been implemented in hydrogel cross-linking. The inherent reversibility of metal–ligand coordination renders the resulting hydrogels as shear-thinning and self-healing. While catechol–Fe^{3+}[79,80] and histidine–Ni^{2+}[81] are some common metal–ligand complexes used previously, many other complexations exist and offer a unique opportunity to form radiopaque hydrogels utilizing the coordination between heavy metals and polymers.[71] Nanocomposite hydrogels have also been formed where polymer chains are physically cross-linked to assemble with nanoparticles or nanostructures.[82] Various nanoparticles such as carbon nanotubes, silicates, and metal/metal oxide nanoparticles can be combined with polymers to obtain nanocomposite hydrogels.[83] In addition to physical incorporation of nanoparticles into hydrogel systems,[84] recent studies have highlighted the use of nanoparticles as cross-linkers.[85] Along with metal coordination, nanocomposites offer significant potential in the formation of radiopaque hydrogels, particularly as nanoparticles can be used for both cross-linking and radiopacity.

Hydrophobic associations play a critical role in the formation of hydrogels via physical associations and usually involve incorporation of hydrophobic domains into polymers for

self-assembly. Peptide amphiphiles and amphiphilic block copolymers rely largely on these hydrophobic associations and are reviewed elsewhere.[86–88]

2.2. Chemical Cross-Linking.

Chemical cross-linking relies on covalent bonding between polymer chains. When compared to physical interactions, chemical cross-linking generally increases hydrogel stability and mechanical properties and allows enhanced control of variables such as gelation time and degradation properties. There are numerous types of chemical reactions that are employed to form hydrogels, including radical polymerizations, thiol–ene cross-linking, Michael addition reactions, and enzymatic cross-linking. Each approach uses specific reactive groups and has their own advantages in the formation of biomedical hydrogels.

Radical chain polymerizations involve formation of a radical through an initiator and initiation source (e.g., light, temperature, redox reaction), which then reacts with functional groups on molecules to form polymers. Acrylates and methacrylates are the most common reactive groups used in radical polymerizations,[89] and a wide variety of initiators have been used, such as photoinitiators and the ammonium persulfate (APS)/ tetramethylethylenediamine (TEMED) system as a common nonlight-activated initiator/ accelerator system. Many synthetic (polyanhydrides, PEG, polypropylene fumarates, poly(α-hydroxy esters), PVA) and natural (HA, dextran, chitosan, chondroitin sulfate) polymers have been functionalized with reactive groups to render them crosslinkable into hydrogels using radical polymerizations and have been explored for a variety of biomedical applications.[90] While this method allows rapid and robust hydrogel formation, the polydispersity in kinetic chains and cross-linking density results in heterogeneous networks.[91]

Light-activated free-radical cross-linking has gained particular interest in biomedical applications due to its temporal and spatial control of reactions and potential for *in situ* gelation.[92] Photo-cross-linking can be carried out at physiological temperatures and pH, enabling their use in minimally invasive surgical procedures.[93] Photo-cross-linking of biomedical hydrogels is achieved via a photoinitiator and irradiation at adsorption wavelengths to generate radicals.[92] These radicals attack carbon–carbon double bonds on precursor macromolecules, forming covalent bonds that cross-link into a network rapidly upon light exposure. A variety of photoinitiators are commercially available and continue to be developed.[94]

Thiol–ene photo-cross-linking, a reaction between a thiol and an alkene (e.g., norbornene) in the presence of light and a photoinitiator, represents a different mechanism involving step-growth of a network.[95] Combining the advantages of both radical polymerization and bio-orthogonal click reactions, thiol–ene photo-cross-linking has enhanced control of network homogeneity. Furthermore, unlike other photo-cross-linking techniques, thiol–ene reactions are not inhibited by the presence of oxygen. As an example, the thiol-norbornene reaction has been used extensively to form,[96] photopattern,[97] and further functionalize[98] hydrogels with peptides, proteins, and small molecules.

Michael addition reactions involve the nucleophilic addition of thiol- or amine-bearing molecules to an α-β-unsaturated carbonyl compound (e.g., acrylates, methacrylates, vinyl sulfones).[99] Compared to chain growth polymerizations, step growth reactions allow more homogeneous network structures and offer a simple strategy to incorporate functional peptides into hydrogels.[91] Michael addition reactions between thiols and acrylates/vinyl sulfones have been extensively used for the *in situ* formation of hydrogels due to the reaction's mild conditions, tunability, and high chemical yield. Since Elbert et al.'s early study on protein delivery,[100] many PEG-, HA-, and dextran-based hydrogels have been formed via Michael addition reactions for drug delivery applications.[101–104] Recently, divinyl sulfone-,[53] carbazate and aldehyde-,[105] and thiol- and diacrylate-[52] modifications have been utilized to form imageable hydrogels via this reaction.

Enzymatic cross-linking has emerged as an approach to form *in situ* hydrogels due to mild reaction conditions.[106] Transglutaminases,[107] peroxidases,[108] and tyrosinases[109] have been reported for cross-linking hydrogels. Horseradish peroxidase (HRP) has been particularly attractive for hydrogel formation, whereby cross-linking is induced by the addition of hydrogen peroxide to solutions of tyramine-modified monomers after which phenolate radicals isomerize and dimerize to form C–C bonded dityramine adducts. Tyramine-modified gelatin has been recently functionalized with AuNP and cross-linked with HRP.[110]

Dynamic covalent bonds are able to be formed, broken, and reformed, either autonomously or under stimuli. These dynamic properties are particularly attractive as hydrogels are being developed for minimally invasive clinical applications. Compared to physical associations, dynamic covalent reactions have slower kinetics of bond cleavage and formation, giving rise to more stable materials while still allowing injectability.[111] Schiff base reactions including imine derivatives (between amine and aldehyde groups) as well as hydrazone bonds (between aldehyde and hydrazide groups) have been used extensively for tissue engineering and drug delivery applications.[112] Oxime bonds, formed through the condensation of hydroxylamine with a ketone or aldehyde, exhibit improved hydrolytic stability over hydrazones and imines.[113,114] Disulfides, formed by the reaction of two thiol groups, require the presence of an oxidation agent to form and can be broken down or reform via physiologically relevant reduction/oxidation reactions.[115,116]

3. FUNCTIONALIZED IMAGEABLE HYDROGELS

Several approaches have been developed to render hydrogels detectable by various imaging techniques without affecting their rheological properties and biocompatibility, while limiting their synthetic complexity. These include hydrogels that are intrinsically imageable or where the hydrogel is rendered imageable via the encapsulation of contrast agents via dynamic interactions (e.g., ionic interactions, H-bonding) or by the formation of covalent or coordination bonds with contrast agents (Figure 1). In this section, we review the methods of functionalizing imageable hydrogels with a particular emphasis on methods used to incorporate imaging features for biomedical applications, and the formulations used for such purposes are summarized in Table 3.

3.1. Intrinsically Imageable Hydrogels.

Hydrogels can display intrinsic contrast in medical imaging without the need for orthogonal functionalization with a probe, such as semiconducting organic polymers that are fluorescent,[147] carbonyl-containing hydrogels that universally present autofluorescence,[120] and polyaromatic networks that display aggregation-induced emission in optical imaging.[148] Although the monitoring of label-free hydrogels requires sophisticated design to access polymers or small molecules that display high fluorescence quantum yield or near-infrared (NIR) optical properties and to understand complex relationships between changes in signal and hydrogel quantity, this approach holds significant benefits since it does not typically require modification of the hydrogel formulation for imaging. As an example, biocompatible polyester oligomers can be obtained by enzymatic catalyzed transesterification and can be further cross-linked with polytopic polyethyleneglycol acrylates to afford hydrogels displaying intrinsic fluorescent contrast and eventually degrade via ester bond hydrolysis.[121]

On the other hand, hydrogels bearing exchangeable protons (e.g., protons involved in a covalent bond with a heteroatom such as hydroxy-, amino-, or amido- functions) can be visualized by chemical exchange saturation transfer (CEST), which is an approach in MRI that requires exchangeable protons that can be saturated and transferred for indirect detection through changes in the water signal.[52,117] For example, pemetrexed (Pem), can be functionalized with a rationally designed peptide and enable its self-assembly by π–π stacking interaction into a filamentous hydrogel that display intrinsic contrast in CEST-MRI.[118]

3.2. Physical Loading of Contrast Agents.

Contrast agents that are physically loaded into hydrogels are typically retained via hydrogen bonding, coordination bond, ionic, hydrophobic, or other noncovalent interactions, or simply physically restrained in covalently cross-linked hydrogels.[129,145,149,150] The procedure of physical loading of contrast agents in the hydrogel is either via incubation with preformed hydrogels by passive diffusion through the network or entrapment in the hydrogel during formation. Such a strategy allows a wide range of chemical entities to be loaded into the hydrogel, leveraging the extensive developments in the field of contrast agents with a multitude of probes with excellent properties in terms of strong contrast production, high stability, and chemical diversity. The simplicity of this approach also allows excellent contrast properties for medical imaging without the need for new chemical compositions. Polymers with chelating ability, such as polytopic alginate, can be cross-linked with several cationic metals, e.g., ^{111}In and ^{89}Zr, that are active in single photon emission computed tomography (SPECT) or positron emission tomography (PET) imaging, affording hydrogels that can be tracked *in vivo*.[63] This approach has been used to monitor oral drug delivery to the stomach in the form of metal cross-linked alginate based oral formulations and as cross-linked hydrogel suspensions for nasal administration of small molecules to facilitate their delivery to the brain. Additionally, some nanoparticles such as gold nanoparticles (AuNP) can be assembled via supramolecular interactions to form a hydrogel with potential for biomedical applications.[151] This approach is especially useful as they are well established contrast agents in CT, photoacoustics, and other imaging modalities.[56,152–154] Aggregation is possible for nanoparticle-based contrast agents such as AuNP, which might lead to

unwanted retention in tissues and toxicity.[155] To prevent aggregation, capping agents such as thiol-terminated polyethylene glycol (PEG) is commonly used to functionalize the surface of AuNP in order to improve their *in vivo* stability and to avoid uptake by the reticular endothelial system (RES).[156] Besides, other factors such as hydrogel pH and nanoparticle concentration can also contribute to the possibility of aggregation, and these factors should be taken into consideration when formulating contrast agent loaded hydrogels. Additionally, upconverting nanoparticles (UCNP) and fluorescent dyes (e.g., indocyanine green (ICG) and methylene blue (MB)) are of particular interest in optical imaging. For instance, a chitosan-HA hydrogel cross-linked with β-glycerophosphate and genipin and loaded with $LiYF_4:Yb^{3+}/Tm^{3+}$ UCNP can be monitored by optical imaging using NIR excitation.[157] A nanofiber hydrogel formed by self-assembly of the melittin peptide could be loaded by physical mixing with ICG and be detected by both photoacoustic imaging and NIR fluorescence.[133] Additionally, m-ferrite nanoparticles, gadolinium chelates, and iron oxide nanoparticles have been physically loaded in various hydrogel formulations and be detected by MRI.[20,32,158,159]

One drawback of long-term *in vivo* monitoring of the morphology and degradation of hydrogels that are physically loaded with contrast agents is that the passive diffusion of the agents from the hydrogel may occur. This can result in gradients of the contrast agents from the surface to the center of the hydrogel, leading to possible underestimation of hydrogel volumes. However, multiple reports have addressed this by investigating the contrast agents' elution from hydrogels in *in vitro* or *ex vivo* models and have developed mathematical models to predict this phenomenon in living systems or designed hydrogels to limit the passive diffusion of the contrast agent.[132,148,160] Furthermore, physical loading can allow the same hydrogel to be imaged with different medical imaging modalities, simply by using multiple contrast agents that leverage different imaging modalities. This can be of particular interest when switching from use in superficial to deeply located tissues due to the varying depth penetration of imaging techniques and has been used with a range of contrast agents, including small probes active in fluorescence[112,161] or aggregation induced emission,[148] metal complexes monitored by PET/CT[162] or MRI,[20] and nanosized contrast agents including metal nanoparticles,[16,36,157,163] proteins,[164] or inorganic assemblies.[132]

3.3. Chemical Grafting of Contrast Agents.

Another strategy for hydrogel visualization *in vivo* is the chemical grafting of contrast agents to the hydrogel via a covalent bond.[33,142,160,165–168] The chemical grafting of contrast agents has potential for monitoring both the hydrogel degradation and elimination route, which is valuable for biodegradable hydrogels. One of the factors that is critically important for monitoring hydrogels *in vivo* is the longevity of the contrast generation from the hydrogels. Unlike loading contrast agents through physical loading, the formation of a high-energy bond (e.g., a covalent bond) renders the leaching of the contrast agent from the hydrogel unlikely, thereby increasing the accuracy of quantifying remaining hydrogel. Furthermore, functionalization with a contrast agent by stimuli-responsive bonds, or so-called dynamic covalent bonds, enables the monitoring of stimuli-triggered degradation or payload delivery.

For instance, mPEG-PLA can be functionalized with 2,3,5-triiodobenzoic acid (TIB) by an ester bond enabling the formation of a thermogellable hydrogel that displayed strong radiopacity in CT.[169] The formation and biodegradation of hydrogel obtained by thermogellation of micelles composed of amphiphilic poly(*ε*-caprolactone-*co*-1,4,8-trioxa[4.6]spiro-9-undecanone)-*b*-poly(ethylene glycol)-*b*-poly(*ε*-caprolactone-*co*-1,4,8-trioxa[4.6]spiro-9-undecanone) (PECT) can be imaged with fluorescence resonance energy transfer (FRET) in real-time.[170]

However, fabricating contrast agent functionalized hydrogels through covalent bonds involves sophisticated chemical reactions and purification processes, as opposed to the straightforward approach of physical loading of contrast agents. By covalently introducing contrast agents into the hydrogels, the chemical structure is modified, thereby influencing the properties of hydrogels.[17] For example, covalent linkage of iodine moieties to thermogelling hydrogels to allow tracking with X-ray based imaging could reduce their gelation threshold to below body temperature or create a sol–gel transition that results in phase separation in living systems.[169,171] Thus, efforts have been made to avoid significant effects on their physical gelation properties by finding a specific grafting site on polymers or maintaining a low chemical modification proportion.[17]

Overall, we herein described three approaches to access hydrogels that can be visualized and monitored *in vivo*, including the rational design of intrinsically imageable hydrogels, physical loading of contrast agents by passive diffusion or entrapment in the hydrogel during the gelation process, or functionalization of the hydrogel with contrast agents by covalent bonds. These three strategies each offer different advantages, such as circumventing the need for labeling in the case of intrinsically imageable hydrogels, the ability to load a wide array of payloads in physical loading, or better correlation of signal with residual hydrogel in chemical grafting. Yet, they each suffer from limitations, for example, there is a relatively small number of intrinsically imageable hydrogels, while physical loading decouples signal from hydrogel erosion and chemical grafting has effects on mechanical properties. Hence, the different strategies offer complementary benefits and limitations that must be considered when selecting the best strategy for an individual application.

4. APPLICATIONS OF HYDROGEL IMAGING

There are numerous modalities used for biomedical imaging applications, but only a subset of them are widely used for hydrogel imaging. Considering several parameters, such as penetration depth, image resolution, source of contrast, and the goal of the imaging, the most relevant imaging modalities are largely CT, MRI, fluorescence imaging, and several other less commonly used modalities, such as nuclear imaging, photoacoustic imaging, and ultrasound.[172] These imaging modalities, with the exception of photoacoustics and fluorescence imaging, are extensively utilized as diagnostic tools in clinical settings, and each of them has their own advantages and limitations. For example, CT is much faster and considerably lower cost than MRI, and it allows for accurate detection of calcified structures.[173,174] On the other hand, MRI does not use ionizing radiation and has a much greater range of available soft tissue contrast and higher anatomical resolution.[175]

In this section, the principles of several imaging technologies and their hydrogel imaging applications will be reviewed and discussed.

4.1. X-ray Imaging.

4.1.1. X-ray Imaging Principles.—X-ray imaging was the first medical imaging modality, being invented in 1895. Despite its age, it is still by far the most widely used imaging technique and sees ubiquitous clinical use throughout the world. Moreover, it is an accessible, economical, and a widely used research tool, of particular value in imaging bones and joints, which are two of the organs for which there is the greatest interest in using hydrogels for tissue regeneration. Such advantages grant radiopaque hydrogels good potential for future clinical translation, and X-ray imaging of hydrogels is of considerable interest. X-rays are a form of electromagnetic radiation that is typically produced by two mechanisms, namely, Bremsstrahlung radiation and characteristic radiation.[176,177] There are several imaging modalities that use X-rays, including planar X-ray imaging that provides 2-dimensional images of objects such as fractured bones or the gastrointestinal tract;[178] CT which uses rotating X-ray sources to generate 3-dimensional images of anatomy;[179] fluoroscopy that uses mobile X-ray sources to obtain real-time moving images of anatomy;[180,181] SPCCT for material-specific multi-contrast imaging;[182,183] and mammography for breast imaging.[184]

Despite the fact that X-rays are used differently in these modalities, the principles of X-ray contrast generation are similar for each. An X-ray beam's intensity is reduced as it traverses matter, as a result of tissue absorption or scattering of X-rays.[185] However, most soft tissues are difficult to distinguish on the basis of the contrast produced by the tissues themselves, since they are all composed of similar, weakly attenuating elements.[179,186] Meanwhile, hydrogels, with water as their main component and polymers that are usually made up of elements close in atomic number to organic materials, tend to produce contrast that is indistinguishable with soft tissues.[187] As a result, X-ray contrast agents typically need to be embedded in hydrogels in order to differentiate hydrogels from adjacent tissues.

X-ray contrast agents are typically biocompatible, water-soluble, and highly stable in aqueous media, and such properties are beneficial to make them compatible with hydrogels.[154,188] A wide array of X-ray contrast agents have been utilized in X-ray hydrogel imaging, namely, AuNP,[110,123–125] tantalum oxide microparticles,[31] platinum nanoparticles (PtNP),[126] barium sulfate suspensions,[127] and iodine molecules.[128,189,190] Among these, barium sulfate suspensions and iodinated small molecules are the only contrast agents that are currently FDA-approved, although the other agents are either heavily investigated preclinically or in clinical trials.[41,191] For a hydrogel labeled with one of the FDA-approved agents, an easier translation of the approach to the clinic could be achieved. However, iodinated small molecules may rapidly leave the hydrogel, thus providing only a relatively short period of contrast during which the hydrogel can be monitored. On the other hand, non-FDA approved contrast generating materials such as AuNP will typically remain entrapped in the hydrogel longer, thereby allowing the hydrogel to be monitored for a long duration in preclinical settings. Barium sulfate suspensions, while FDA-approved, are

designated for oral use and if administered via injection or surgically may never be cleared from the body, which would be a concern for clinical use.

4.1.2. Radiopaque Markers.—The encapsulation of these contrast agents in hydrogels is critical to the enhancement of hydrogel radiopacification, and numerous studies have demonstrated the use of such radiopaque hydrogels in different biomedical applications. For instance, radiopaque hydrogels have been used as radiopaque markers, known as fiducials, to aid with targeting of local therapy and radiographic localization of tumors and normal tissues.[192] Indeed, a PEG hydrogel containing covalently bound iodine has been approved by the Food and Drug Administration (FDA) for this purpose.[193] This radiopaque PEG hydrogel was designed to identify the lumpectomy cavity during oncoplastic breast-conserving surgery with a CT scan, thus improving radiotherapy target definition in the lumpectomy cavity.[194] Similarly, it has been repurposed to visualize targets via CT scanning during brachytherapy in gynecologic malignacies[193] and during minimally invasive thoracic surgery in thoracic malignancies.[192]

4.1.3. Wound Healing.—Alternatively, radiopaque hydrogels can play important roles in wound healing, for instance, to prevent postoperative adhesions (painful internal scarring). Lei et al. developed a thermoreversible injectable PET/polyester hydrogel with X-ray opacity. The system was fabricated based on mixing monomethoxyl poly(ethylene glocol)-poly(D,L-lactic acid-*co*-glycolic acid) (mPEG-PLGA) deblock copolymer with is 2,3,5-TIB end-capped derivative. The performance on the prevention of postoperative adhesions was evaluated using a rat model with cecum and abdominal defects. The animals underwent sequential CT scans during the week after receiving the treatment of the radiopaque thermoreversible hydrogels, and the hydrogels can be clearly observed in the abdomen and distinguished from the surrounding soft tissues from sectional views of the scans and reconstructed 3-D models at various time points (Figure 2A,B).[171]

4.1.4. Tissue Engineering.—In addition to wound healing applications, tissue engineering is another field that can benefit from radiopaque hydrogels, whereby effective imaging methods can be used to evaluate new tissue formation and the fate of scaffolds. Hydrogels such as gelatin methacrylate are widely used for tissue regeneration owing to their ability to induce the formation of extracellular matrix. AuNP embedded gelatin hydrogels showed evident osteogenic features and were used to evaluate bone formation in bone regeneration.[125] More recently, a radiopaque alginate hydrogel formed by substituting calcium ions with barium ions for cross-linking was fabricated, which provided information on the rate of implant degradation and thus showed great potential as tissue engineering constructs.[195]

In the case of hydrogel imaging, the low sensitivity of X-ray imaging methods does not usually present a problem, since it is straightforward to load hydrogels with sufficient contrast generating material to render them easily visible compared to soft tissues. In the case of highly attenuating tissues such as bone, new multienergy based X-ray imaging methods offer the ability to distinguish hydrogels that contain payloads such as AuNP via “k-edge imaging”. Indeed, in the context of hydrogel imaging, aspects of X-ray imaging that are sometimes viewed as a weakness, such as the lack of soft tissue contrast, can be a

strength, since there should be no uncertainty as to the signal arising from the hydrogel. In comparison, for MRI, which provides a lot of soft tissue contrast, hydrogel administration can lead to scarring, an influx of inflammatory cells, and tissue movement, all of which can lead to contrast that may confound efforts to monitor the hydrogel. An additional strength of X-ray imaging is the linear correlation between signal and concentration, which is not the case for other methods such as fluorescence or MRI.

Another benefit for X-ray imaging is that FDA-approved iodinated contrast agents often have chemical groups that can be used for covalent attachment to hydrogels. Therefore, hydrogels can either be physically loaded or chemically grafted with these agents. Overall, X-ray imaging is an ascendant technique to evaluate the performance and degradation of tissue implants or to assess drug delivery.

4.2. MRI Imaging.

4.2.1. MRI Imaging Principles.—MRI imaging makes use of a strong magnetic field (e.g., 0.2–7 T) in which hydrogen nuclei in water molecules are forced to align. These protons are excited by application of radiofrequency (RF) pulses and return to equilibrium, referred to as relaxation, once the RF signal ceases. The RF signal emitted from the nuclei as they relax is recorded to reconstruct images. Pulse sequences can be developed to focus on longitudinal relaxation(i.e., T_1 relaxation) or transversal relaxation (i.e., T_2 relaxation), which results in T_1-weighted or T_2-weighted images, respectively.[175,196] Unlike CT where tissue contrast mainly depends on electron density, contrast in MRI is a complex function of proton density, T_1 relaxation, T_2 relaxation, and local chemical environment.[197] The majority of MRI contrast agents are either paramagnetic (i.e., gadolinium ion complexes and manganese chelates), which are used for T_1 weighted imaging or superparamagnetic (i.e., iron oxide nanoparticles).[198] On the other hand, CEST imaging, a relatively new MRI contrast approach, enables certain endogenous compounds containing protons exchangeable with surrounding water molecules to be directly detected.[199,200]

To render MRI-visible hydrogels, FDA-approved gadolinium chelates can be physically loaded into hydrogels. While there have been reports of covalent grafting of gadolinium chelates, this has to be done with chemically modified gadolinium chelates.[139] This chemical modification leads to two drawbacks. First, the chelate is no longer an FDA-approved entity, limiting translation. Second, gadolinium chelates are structures that are very carefully engineered to tightly bind gadolinium and prevent the release of this toxic ion. Modification of the structure can compromise the stability of the chelate. Moreover, given the concerns over gadolinium safety, such as nephrogenic systematic fibrosis and gadolinium brain retention, the approval of using a hydrogel in patients that is effectively a long-residing depot of gadolinium will face significant hurdles. Alternatives for MR imaging of hydrogels include labeling with iron oxide nanoparticles and CEST imaging. There are FDA-approved iron oxide nanoparticles, which is a benefit for clinical translation, but only ferumoxytol is still currently on the market. Additionally, there has only been one report to date of labeling hydrogels with this agent which points to challenges in incorporating ferumoxytol into hydrogels.[130] An additional challenge for labeling hydrogels with iron oxides is that they cause signal loss in MR images. However, there can be many factors

that result in signal loss in MRI, such as gas or hemorrhages, therefore a site of contrast cannot be definitively ascribed to the presence of hydrogel. CEST is attractive as a label-free approach for hydrogel imaging, although it is limited to hydrogels that have appropriate exchangeable protons and the contrast yielded by CEST is typically quite modest. Moreover, for all types of approaches to imaging hydrogels with MRI, contrast is not directly correlated to concentration, which is a limitation for quantification and monitoring degradation. Nevertheless, MRI can be used to form images of exceptional quality and the ability to use natural or various FDA-approved materials for CEST MRI is appealing.

4.2.2. Conventional MRI.—One of the earliest efforts to visualize hydrogels using MRI with gadolinium contrast agents was reported by Courant et al.[140] Gadolinium complexes were encapsulated in chitosan and HA-based hydrophilic polymer matrix and exhibited contrast generation in T_1- and T_2-weighted images. Since then, monitoring hydrogel degradation using MRI has been extensively studied. Gadolinium complexes were modified with dithiopyridyl groups and used to label an HA derivative for longitudinal tracking *in vivo*.[139] *In situ* forming hydrogels are also of great interest in tissue regeneration as "MRI reporter gels", which serve as smart and responsive polymer implants to deliver drug *in vivo* and are evaluated by MRI over time. A pH sensitive, injectable, and self-healing chitosan-based hydrogel functionalized with gadolinium chelate was able to self-heal within a pH range based on Schiff-base linkages (Figure 3 A). *In vivo*, the hydrogels were injected into rats subcutaneously and could be detected on T_1-weighted MRI upon injection and at 35 days after injection with declining intensity (Figure 3B,C).[32] Similarly, a supramolecular *in situ* forming ureidopyrimidinone (UPy)-based hydrogel was functionalized with a gadolinium-DOTA complex for monitoring treatments postmyocardial infarction, where sequential measurements of specimens to determine structure, location, and degradation could be also achieved.[48] Alternatively, iron oxide nanoparticles have been investigated for visualizing hydrogels in tissue engineering and drug delivery as well. For example, ultrasmall superparamagnetic iron oxide nanoparticles (SPIONs) were labeled on cellulose nanocrystal/silk fibroin-blended hydrogel system to monitor hydrogel degradation during cartilage regeneration.[16] The same SPIONs were incorporated into the dehydrodipeptide-based hydrogels. Upon magnetic excitation, the SPIONs were able to generate a significant amount of heat achieving magnetic hyperthermia, which can be used as a remote trigger for drug releases from hydrogels.[131]

4.2.3. CEST MRI.—On the other hand, as mentioned previously, hydrogels can be characterized *in vivo* using CEST MRI if they have exchangeable protons. CEST imaging has the unique benefit of allowing the evaluation of hydrogels without the need of metal-based contrast agents, which can potentially lead to side effects such as nephrogenic systemic fibrosis.[201] Fortuitously, there are polymers that are CEST active and also FDA-approved. For example, HA and gelatin-based hydrogels are readily detectable with CEST MRI as they are rich in exchangeable protons, and they are of particular interest due to this reason. Dorsey et al. reported injectable HA hydrogels and illustrated the CEST signal tuning by manipulating hydrogel properties (i.e., macromer concentration) (Figure 4A).[119] Subsequently, Shazeeb et al. assessed the degradation profiles and residence time of chemically cross-linked HA hydrogels with CEST MRI *in vivo*. The CEST signal showed

a gradual decrease with time in response to the degradation of the hydrogels (Figure 4B,C), and a loss in CEST contrast indicated degradation, as supported by histology performed at the end of study.[53]

Furthermore, taking advantage of the presence of an exchangeable aromatic amine proton with a chemical shift of 5.2 ppm in the backbone of pemetrexed (Pem, an FDA-approved chemotherapeutic that is highly hydrophobic) and loading this drug through π–π stacking interactions yielded a filamentous hydrogel that has intrinsic contrast in CEST-MRI (Figure 5A–D).[118] This approach enabled a high drug content of 42% for glioma therapy and was used to visualize the injected hydrogel and monitor its degradation. The gradient-driven release of the drug to the surrounding tissues was visible up to 4 days postinjection and could be quantified by CEST-MRI.

Thus far, several other studies have taken advantage of CEST MRI for label-free imaging of hydrogels.[118,202,203] This method is particularly appealing as it does not perturb the intrinsic MR properties of native tissues and provides a practical approach to visualize polymer-mediated drug delivery without the use of imaging probes. Overall, MRI has been demonstrated to allow *in vivo* hydrogel assessment in several settings, and there is the option to use either exogenous contrast agents or intrinsic imageable materials (in certain cases). However, the wide use of MRI for hydrogel imaging is limited by its high cost, long scan times, and need for technical expertise compared to other methods such as X-ray and CT.

4.3. Fluorescence Imaging.

4.3.1. Fluorescence Imaging Principles.—Fluorescence imaging is a type of noninvasive imaging technique that can be used to study a wide variety of molecular entities in both living cells and *ex vivo* tissue samples, via fluorescent probes. The use of NIR wavelengths (i.e., 650–900 nm) has advantages over visible-range light, including relatively deep photon penetration into tissues, less tissue autofluorescence, and higher optical contrast when exogenous NIR fluorophores are introduced.[204] Coupled with advances in detectors and dye technologies, it offers exceptional visual monitoring of life processes with relatively minimal perturbation to biological samples.[56,205,206] To date, clinical applications employing NIR fluorescence are being explored and range from assessing blood flow and detecting sentinel lymph nodes to visualizing tumor lesions, with the help of nonspecific or specific fluorescent agents.[207] Fluorescent materials such as quantum dots, small molecule fluorophores, intrinsically fluorescent polymers or proteins that emit light upon excitation can be used in fluorescence imaging.[208,209] Fluorescent hydrogels differ from conventional hydrogels in their light emitting properties but retain their extended polymeric networks. Hydrogels can have fluorescent properties due to the polymer of choice or via physically loaded fluorescent materials.[210] The drawbacks of fluorescence imaging include the low penetration depth, complex relationships between signal and concentration, and absence of FDA-approved fluorescence imaging systems.

4.3.2. Drug Delivery.—As an example of hydrogels with intrinsic fluorescent contrast, biocompatible polyester oligomers obtained by enzymatic catalyzed transesterification were cross-linked with PEG acrylates due to the intrinsic autofluorescence of sericin polypeptide,

with high quantum yields ranging from 16.42% to 36.41%.[121] The hydrogel degraded via ester bond hydrolysis, which could be monitored noninvasively after subcutaneous injection in nude mice via fluorescence imaging under 488 nm excitation and 520 nm emission wavelength. Additionally, this intrinsically imageable hydrogel successfully enabled the delivery of various payloads, highlighting its potential for theranostic and drug delivery applications. As another example in drug delivery, a nanofiber hydrogel formed by the self-assembly of the melittin peptide was loaded with 1% w/w of indocyanine green (ICG), which is an optically active small molecule, without affecting its rheological properties (Figure 6A,B). This hydrogel was detected *in vivo* by photoacoustic imaging and NIR fluorescence (Figure 6C) and displayed strong tumor growth inhibition activity against glioblastoma by photothermal therapy.[133] This strategy has found a broad application in the field of drug delivery, enabling both the coloading of two or more contrast agents and drugs and monitoring the *in vivo* drug release by the decrease in contrast in the hydrogel over time.[36,146,211,212]

4.3.3. Implant Monitoring.—Similar to other imaging modalities as mentioned earlier, fluorescent hydrogels have been explored for monitoring implants and other theranostic applications. Indeed, hydrogels conjugated with upconversion nanoparticles (UCNPs) have been reported for long-term *in vivo* tracking of the distribution and degradation of hydrogels.[61] Besides their fluorescent properties, UCNPs can be used for photodynamic therapy (PDT) and photothermal therapy (PTT) for cancer, as they can activate surrounding photosensitizer molecules to generate reactive oxygen species and heat to kill tumor cells.[213] The combination of UNCPs and hydrogels can therefore not only act as tumor imaging probes but also serve as therapeutic agents. For instance, doxorubicin-loaded gelatin hydrogels containing UCNPs were used for antitumor chemophotothermal therapy and upconversion fluorescence imaging.[135] Similarly, an injectable silk fibroin nanofiber hydrogel hybrid system was developed for tumor upconversion luminescence imaging and photothermal therapy.[136] Apart from UCNPs, fluorophores can be used to give hydrogels fluorescent properties as well. Park et al. engineered fluorescent HA and gelatin-based hydrogels by conjugating an 800 nm indocyanine NIR fluorophore ZW800-3a through its carboxylic functional group to the amine groups in gelatin (Figure 7A).[33] They were able to simultaneously monitor scaffold degradation and brain tissue regeneration by imaging the hydrogel using the 800 nm channel and observing brain tissue ingrowth with the 700 nm channel, by use of a 700 nm active brain-specific contrast agent (Figure 7B). Furthermore, others have shown the incorporation of different fluorescent probes in hydrogels for similar purposes in hydrogel tracking, drug delivery, and fluorescence-guided surgery.[122,132,142]

4.3.4. Biosensors.—Hydrogels themselves also have drawn attention as biosensors as they can respond to external stimuli. For instance, when interacting with target analytes, they can undergo physical changes, which can be monitored by observing the hydrogel deformation.[214] However, directly observing such changes *in vivo* is challenging. To this end, fluorescent hydrogels find advantages as biosensing platforms by producing changes in fluorescence signal generated by chemical reactions.[215] Kim et al. presented a self-assembled, photoluminescent peptide hydrogel consisting of *N*-fluorenyl-methoxycarbonyl diphenylalanine (Fmoc-FF) for detection of analytes, such as glucose and

phenolic compounds, via coencapsulation of enzymes as bioreceptors and quantum dots as fluorescent reporters.[134] Similarly, glucose-responsive PEG-bonded polyacrylamide (PAM) fluorescent hydrogel fibers were used for long-term *in vivo* glucose monitoring, and they could continuously respond to blood glucose concentration changes for up to 140 days.[141] Selective and rapid fluorescence sensing of iron ions with detection limit of as little as 0.228 ppm could be achieved with a chitosan-based fluorescent hydrogel, which is valuable since iron ions are one of the most important and abundant metal ions in the human body. Additionally, fluorescent hydrogels have also been used to detect microRNA,[216] bacteria,[217] proteins,[218] and heavy metal ions.[219]

4.4. Other Imaging Modalities.

In addition to the imaging modalities mentioned above, there are instances of hydrogels imaged via modalities such as nuclear imaging, photoacoustic imaging, and ultrasound, although this is less common. Nuclear imaging is a specialized form of radiological imaging which uses radioactive materials (i.e., radiotracers) to examine the body. Unlike X-ray or CT imaging that use ionizing radiation from an external source, nuclear imaging relies on ionizing radiation sources inside the body, which are then detected by a gamma camera.[220] By radiolabeling hydrogels or incorporating radiotracers in hydrogels, several biomedical applications can be achieved.[143] Kim et al. developed a radiolabeled chitosan-based vascular endothelial growth factor (VEGF) delivery system for acute myocardial infarction.[35] Stuckey et al. incorporated the radio-metal indium-111 into the alginate hydrogels, enabling *in vivo* imaging of hydrogel delivery and retention.[63] In addition, aiming at the important roles hydrogel dressings play in wound care, Op't Veld et al. used polyisocyanopeptide (PIC) thermosensitive hydrogel labeled with indium-111 to facilitate and monitor wound healing using SPECT/CT imaging. It was discovered that the hydrogel can stay localized at the site of application (i.e., the wounds and surrounding skin) for at least 7 days and generate a consistent signal (Figure 8).[145]

4.4.1. Nuclear Imaging.—Nuclear imaging of hydrogels provides advantages of high sensitivity and specificity. However, as mentioned above, hydrogel applications often do not need such high sensitivity since they are concentrated depots of material. Moreover, a radiolabeled hydrogel represents significant logistical challenges related to safety, both from the perspective of material preparation and animal handling over a protracted period. In addition, while nuclear imaging is widely used in the clinic, this is mostly with relatively short-lived isotopes. The long-lived isotopes needed for longitudinal hydrogel monitoring, would present a risk to the health of a patient due to lengthy, continuous radiation exposure. These factors may explain the relative unpopularity of nuclear methods for hydrogel imaging. However, for applications where sensitivity is needed or imaging at only short postadministration is desired, nuclear imaging may be an appealing option.

4.4.2. Ultrasound.—Ultrasound is a diagnostic medical imaging method that uses high-frequency sound waves to produce dynamic images of tissues and blood flow inside the body.[221] Ultrasound is used for many applications and is well-known for its use in viewing the fetus during pregnancy. Such an application is attractive as it does not require the use of radiation like CT.[222] Ultrasound also has advantages of low cost, good soft tissue

contrast, and portability but has drawbacks of requiring sophisticated training for both operation and image interpretation and providing only localized images, as opposed to the whole body imaging of CT or nuclear methods. The emergence of contrast-enhanced ultrasound (CEUS) has broadened its use, especially in cardiac and abdominal imaging as well as evaluation in tissues, tumors, and implants, when combined with ultrasound contrast agents (i.e., microbubbles).[223–225] Imaging of hydrogels can therefore be achieved for different theragnostic purposes. For example, Leng et al. used CEUS to characterize the biodegradation and neovascularization of silk protein hydrogel implants in rats. Both ultrasound and CEUS imaging revealed the change of shape and size of hydrogels over time (Figure 9).[34] In another application, alginate-based hydrogels displayed the ability to self-heal damage triggered by applying ultrasound pulses to disrupt ionically cross-linked hydrogels, enabling on-demand delivery of mitoxantrone for breast cancer therapy. Hydrogels were implanted near breast tumors and showed effective inhibition of tumor growth *in vivo*.[226] Similar ultrasound-mediated self-healing hydrogels were reported elsewhere as well.[64]

4.4.3. Photoacoustic Imaging.—Photoacoustic imaging, or optoacoustic imaging is a hybrid imaging technique based on the photoacoustic effect, where pulsed laser light is applied to the subject, which results in conversion of absorbed optical energy into acoustic energy. With typical optical imaging, the light diffusion limits the spatial resolution in deep-tissue imaging. However, since acoustic waves scatter much less than optical waves in tissue, photoacoustic imaging can generate high-resolution images in both the optically ballistic and diffusive regimen and provide greater tissue differentiation.[227,228] Although this imaging technique has scant availability in clinical practice, it shows great potential in preclinical research. Loading hydrogels with photoacoustically active materials allows their detection with photoacoustic imaging. For example, Cheng et al. reported a pH-responsive chitosan hydrogel encapsulating Prussian blue for photoacoustic imaging-guided photothermal therapy of tumors.[137] The precursors to Prussian blue, namely, ferrous and ferricyanide ions were released in the acidic tumor environment from the hydrogel, allowing the *in situ* formation of Prussian blue in the tumor area, which serves as a photoacoustic contrast agent and a photothermal ablation agent at the same time.

4.4.4. Multimodality Imaging.—Lastly, hydrogel monitoring can be achieved by multimodality imaging, which can help to overcome the limitations of separate techniques as each imaging modality has its own unique strength and intrinsic limitations. For example, a multifunctional hydrogel based on an engineered polypeptide and loaded with Ag_2S quantum dots and paclitaxel was developed for fluorescence/photoacoustic imaging.[36] Alternatively, a thermosensitive magnetic nanoemulsion hydrogel was used for MRI and fluorescence imaging guided thermoablative cancer therapy, while the injection was monitored by ultrasound.[138] In addition, the degradation and biomaterial–tissue-interaction of gelatin hydrogels were investigated *in vivo* with MRI, optical imaging, and PET.[229] Multimodality imaging expands the scope of information that can be collected regarding hydrogel localization, retention, degradation, and activity. For example, CT and MRI offers superior structural imaging, whereas other imaging modalities such as PET and optical imaging could provide information at the molecular level, so that when they are

used together, more detailed anatomical and biological information can be obtained.[230,231] One of the most commonly used combinations are PET/CT scan and SPECT/CT scan, which not only shows anatomic details but also images biochemical or physiological phenomena.[63,143,144,232] Besides, optical imaging usually has poor tissue penetration, but this problem can be mitigated when combined with MRI, CT, or PET imaging, which do not have a tissue penetration limit.[233] Overall, ideally the goal of any multimodal imaging is to provide the localization, extent, and metabolic activity of target tissue, and such a goal applies to hydrogel imaging as well.

5. SUMMARY AND FUTURE OUTLOOK

In the current review, we have highlighted various imaging techniques that can assess and monitor the performance of hydrogels after implantation or injection. Hydrogels can be rendered imageable by using intrinsically imageable polymers, physical loading of contrast agents, or functionalizing with contrast agents by covalent or coordination bonds. Using noninvasive imaging modalities to image hydrogels has offered opportunities to allow for direct access to information about their status *in vivo* and enabled study of the release of therapeutics or encapsulated cell migrations. At present, the mainstream techniques used for imaging hydrogels include CT, MRI, fluorescence imaging, nuclear imaging, ultrasound, or the combination of two or more modalities, and their applications can range from monitoring drug delivery, tissue regeneration, and imaging guided surgery to cancer therapy. Unlike traditional post-mortem assessment of implanted hydrogels with histological methods, *in vivo* imaging allows for longitudinal study of hydrogels without unnecessary animal sacrifices at different points in time, and, in the meantime, offer opportunities for combined imaging and therapy, namely, theranostics. Combining imaging diagnostic and therapeutic capabilities into a single platform can be beneficial to develop more individualized and specific therapies.

Currently, the majority of imaged hydrogels are coloaded with therapeutic agents and contrast generating materials. The resulting hydrogel systems that are capable of diagnosis, drug delivery and monitoring of therapeutic response have been previously well investigated. However, this has the disadvantage that the imaging agent is a proxy for the therapeutic and matching properties between the two is challenging. In comparison, there have so far been few hydrogel systems that are developed where the contrast generating material and the therapeutic are the same entity. Many contrast generating materials, especially nanoparticle-based agents, have inherent therapeutic properties, such as radiosensitization or photothermal heating. Moreover, nanoparticles can be readily converted to be theranostic agents by attaching therapeutic moieties to them, due to their tunable surface chemistry. For instance, therapeutics of various forms such as small molecules, proteins, can be conveniently tethered into nanoparticle-based contrast agents.[234] The formation of all-in-one contrast agent-hydrogel theranostic platforms will likely be a greater focus of investigation in the coming years.

Taking the above concept one step further, if the intention is to image the hydrogel, in an ideal world, the imaging would provide information on the hydrogel structure and the therapeutic entity. This might point to developing hydrogels where the substance that both

generates contrast and provides therapeutic effects is also part of the hydrogel structure itself. For example, a gold nanoparticle could provide both contrast and therapy and be engineered into the polymer backbone or be the cross-linker. Such a hydrogel has rarely been reported and would require quite specific chemistry for the theranostic agent; however, it would enable precise information to be gathered in it *in vivo*.

The fact that imageable hydrogels are usually heavily dependent on contrast agents can be a limitation, as only a relatively small subset of contrast agents are clinically approved and available for use for each imaging modality. For instance, only iodinated small molecules and barium sulfate suspensions are approved and available for CT and gadolinium-chelated contrast agents for MRI. Therefore, ideally using clinically approved contrast agents in hydrogel formulation can bolster the clinical translation of these hydrogels. Similar to contrast agents, there is a limit number of clinically approved hydrogel products for each biomedical application. Currently there are over 30 injectable hydrogel-based products that have been approved by the FDA, and most of them are used in intradermal injections.[235] Thus, the most ideal imageable hydrogel formulation would consist of FDA-approved contrast agents and hydrogels, so that they have a higher chance to be approved and translated into clinics. Nevertheless, carefully designed systems composed either entirely or in part of unapproved materials may also progress toward clinical translation.

Overall, detecting and monitoring hydrogels *in vivo* using imaging techniques provides important information on implantation functional status and is of relevance to numerous clinical applications. We expect to see this field grow and become more routine in the coming years to allow systematic investigations of hydrogels *in vivo* as well as in patients, which will promote future clinical translation of these therapeutic systems.

ACKNOWLEDGMENTS

We thank the National Institutes of Health (Grants R01HL131557, R01HL137365, and R21EB029556) and the American Heart Association (predoctoral fellowship to S.U.) for funding that supported this work. We thank Ananyaa Kumar for her feedback on the manuscript.

REFERENCES

(1). Li J; Mooney DJDesigning hydrogels for controlled drug delivery. Nat. Rev. Mater2016, 1 (12), 16071. [PubMed: 29657852]

(2). Chai Q; Jiao Y; Yu XHydrogels for biomedical applications: Their characteristics and the mechanisms behind them. Gels2017, 3 (1), 6.

(3). Guvendiren M; Lu HD; Burdick JAShear-thinning hydrogels for biomedical applications. Soft Matter2012, 8 (2), 260–272.

(4). Ahmed EMHydrogel: Preparation, characterization, and applications: A review. J. Adv. Res2015, 6 (2), 105–121. [PubMed: 25750745]

(5). Hoffman ASHydrogels for biomedical applications. Adv. Drug Delivery Rev2012, 64, 18–23.

(6). Hu W; Wang Z; Xiao Y; Zhang S; Wang JAdvances in crosslinking strategies of biomedical hydrogels. Biomater. Sci2019, 7 (3), 843–855. [PubMed: 30648168]

(7). Akhtar MF; Hanif M; Ranjha NMMethods of synthesis of hydrogels··· A review. Saudi Pharm. J2016, 24 (5), 554–559. [PubMed: 27752227]

(8). Hennink WE; van Nostrum CFNovel crosslinking methods to design hydrogels. Adv. Drug Delivery Rev2012, 64, 223–236.

(9). Li X; Sun Q; Li Q; Kawazoe N; Chen GFunctional hydrogels with tunable structures and properties for tissue engineering applications. Front. Chem2018, 6, 499. [PubMed: 30406081]

(10). Varaprasad K; Raghavendra GM; Jayaramudu T; Yallapu MM; Sadiku RA mini review on hydrogels classification and recent developments in miscellaneous applications. Mater. Sci. Eng., C2017, 79, 958–971.

(11). Parhi RCross-linked hydrogel for pharmaceutical applications: A review. Adv. Pharm. Bull2017, 7 (4), 515–530. [PubMed: 29399542]

(12). Picchioni F; Muljana HHydrogels based on dynamic covalent and non covalent bonds: A chemistry perspective. Gels2018, 4 (1), 21.

(13). Chakma P; Konkolewicz DDynamic covalent bonds in polymeric materials. Angew. Chem., Int. Ed2019, 58 (29), 9682–9695.

(14). Rodell CB; Lee ME; Wang H; Takebayashi S; Takayama T; Kawamura T; Arkles JS; Dusaj NN; Dorsey SM; Witschey WRT; Pilla JJ; Gorman JH; Wenk JF; Burdick JA; Gorman RCInjectable shear-thinning hydrogels for minimally invasive delivery to infarcted myocardium to limit left ventricular remodeling. Circ.: Cardiovasc. Interventions2016, 9 (10), No. e004058.

(15). Ashrafi K; Tang Y; Britton H; Domenge O; Blino D; Bushby AJ; Shuturminska K; den Hartog M; Radaelli A; Negussie AH; Mikhail AS; Woods DL; Krishnasamy V; Levy EB; Wood BJ; Willis SL; Dreher MR; Lewis ALCharacterization of a novel intrinsically radiopaque drug-eluting bead for image-guided therapy: DC Bead LUMI. J. Controlled Release2017, 250, 36–47.

(16). Chen Z; Yan C; Yan S; Liu Q; Hou M; Xu Y; Guo RNon-invasive monitoring of in vivo hydrogel degradation and cartilage regeneration by multiparametric MR imaging. Theranostics2018, 8 (4), 1146–1158. [PubMed: 29464005]

(17). Lei K; Ma Q; Yu L; Ding JFunctional biomedical hydrogels for in vivo imaging. J. Mater. Chem. B2016, 4 (48), 7793–7812. [PubMed: 32263771]

(18). Ren K; He C; Xiao C; Li G; Chen XInjectable glycopolypeptide hydrogels as biomimetic scaffolds for cartilage tissue engineering. Biomaterials2015, 51, 238–249. [PubMed: 25771014]

(19). Kim JI; Lee BS; Chun C; Cho J-K; Kim S-Y; Song S-CLong-term theranostic hydrogel system for solid tumors. Biomaterials2012, 33 (7), 2251–2259. [PubMed: 22189146]

(20). Gallo E; Diaferia C; Di Gregorio E; Morelli G; Gianolio E; Accardo APeptide-based soft hydrogels modified with gadolinium complexes as MRI contrast agents. Pharmaceuticals2020, 13 (2), 19.

(21). Liguori C; Frauenfelder G; Massaroni C; Saccomandi P; Giurazza F; Pitocco F; Marano R; Schena EEmerging clinical applications of computed tomography. Med. Devices: Evidence Res2015, 8, 265–278.

(22). Pelc NJRecent and future directions in CT imaging. Ann. Biomed. Eng2014, 42 (2), 260–268. [PubMed: 24435658]

(23). Morone M; Bali MA; Tunariu N; Messiou C; Blackledge M; Grazioli L; Koh D-MWhole-body MRI: Current applications in oncology. AJR, Am. J. Roentgenol2017, 209 (6), W336–W349. [PubMed: 28981354]

(24). Kose KPhysical and technical aspects of human magnetic resonance imaging: present status and 50 years historical review. Adv. Phys2021, 6 (1), 1885310.

(25). Bhargava P; He G; Samarghandi A; Delpassand ESPictorial review of SPECT/CT imaging applications in clinical nuclear medicine. Am. J. Nucl. Med. Mol. Imaging2012, 2 (2), 221–231. [PubMed: 23133813]

(26). Blankenberg FG; Strauss HWNuclear medicine applications in molecular imaging. J. Magn Reson Imaging2002, 16 (4), 352–61. [PubMed: 12353251]

(27). Luker GD; Luker KEOptical imaging: current applications and future directions. J. Nucl. Med2007, 49 (1), 1–4. [PubMed: 18077528]

(28). Attia ABE; Balasundaram G; Moothanchery M; Dinish US; Bi R; Ntziachristos V; Olivo MA review of clinical photoacoustic imaging: Current and future trends. Photoacoustics2019, 16, 100144. [PubMed: 31871888]

(29). Klibanov AL; Hossack JAUltrasound in radiology: From anatomic, functional, molecular imaging to drug delivery and image-guided therapy. Invest. Radiol2015, 50 (9), 657–670. [PubMed: 26200224]

(30). Seo J; Kim Y.-s. Ultrasound imaging and beyond: recent advances in medical ultrasound. Biomed. Eng. Lett2017, 7 (2), 57–58. [PubMed: 30603151]

(31). Hong S; Carlson J; Lee H; Weissleder RBioorthogonal radiopaque hydrogel for endoscopic delivery and universal tissue marking. Adv. Healthcare Mater2016, 5 (4), 421–426.

(32). Liu J; Wang K; Luan J; Wen Z; Wang L; Liu Z; Wu G; Zhuo RVisualization of in situ hydrogels by MRI in vivo. J. Mater. Chem. B2016, 4 (7), 1343–1353. [PubMed: 32262990]

(33). Park GK; Kim S-H; Kim K; Das P; Kim B-G; Kashiwagi S; Choi HS; Hwang NSDual-channel fluorescence imaging of hydrogel degradation and tissue regeneration in the brain. Theranostics2019, 9 (15), 4255–4264. [PubMed: 31285760]

(34). Leng X; Liu B; Su B; Liang M; Shi L; Li S; Qu S; Fu X; Liu Y; Yao M; Kaplan DL; Wang Y; Wang XIn situ ultrasound imaging of silk hydrogel degradation and neovascularization. J. Tissue Eng. Regener. Med2017, 11 (3), 822–830.

(35). Kim D-W; Lee C-M; Kim N-H; Lee SY; Lee MY; Choi ES; Park S-A; Kim CG; Hwang H; Lim ST; Sohn M-H; Jeong H-JRadiolabeled chitosan hydrogel containing VEGF enhances angiogenesis in a rodent model of acute myocardial infarction. Macromol. Res2014, 22 (3), 272–278.

(36). Jin R; Yang X; Zhao D; Hou X; Li C; Song X; Chen W; Wang Q; Zhao Y; Liu BAn injectable hybrid hydrogel based on a genetically engineered polypeptide for second near-infrared fluorescence/photoacoustic imaging-monitored sustained chemo-photothermal therapy. Nanoscale2019, 11 (34), 16080–16091. [PubMed: 31432846]

(37). Ehman EC; Johnson GB; Villanueva-Meyer JE; Cha S; Leynes AP; Larson PEZ; Hope TAPET/MRI: Where might it replace PET/CT?J. Magn Reson Imaging2017, 46 (5), 1247–1262. [PubMed: 28370695]

(38). Schneider A; Feussner HChapter 5: Diagnostic Procedures. In Biomedical Engineering in Gastrointestinal Surgery; Schneider A, Feussner H, Eds.; Academic Press, 2017; pp 87–220.

(39). Bybel B; Brunken RC; DiFilippo FP; Neumann DR; Wu G; Cerqueira MDSPECT/CT imaging: Clinical utility of an emerging technology. Radiographics2008, 28 (4), 1097–1113. [PubMed: 18635631]

(40). Hounsfield GNComputerized transverse axial scanning (tomography). 1. Description of system. Br. J. Radiol1973, 46 (552), 1016–22. [PubMed: 4757352]

(41). Yu S-B; Watson ADMetal-based X-ray contrast media. Chem. Rev1999, 99 (9), 2353–2378. [PubMed: 11749484]

(42). Dong YC; Cormode DPHeavy elements for X-ray contrast. In Metal Ions in Bio-Imaging Techniques; Astrid S, Eva F, Roland KOS, Eds.; De Gruyter, 2021; pp 457–484.

(43). Teo SY; Wang SCRadiologic features of polyacrylamide gel mammoplasty. AJR, Am. J. Roentgenol2008, 191 (3), W89–95. [PubMed: 18716084]

(44). Barnett BP; Gailloud PAssessment of EmboGel—A selectively dissolvable radiopaque hydrogel for embolic applications. J. Vasc. Interv. Radiol2011, 22 (2), 203–211. [PubMed: 21185201]

(45). Si-Mohamed S; Cormode DP; Bar-Ness D; Sigovan M; Naha PC; Langlois J-B; Chalabreysse L; Coulon P; Blevis I; Roessl E; Erhard K; Boussel L; Douek PEvaluation of spectral photon counting computed tomography K-edge imaging for determination of gold nanoparticle biodistribution in vivo. Nanoscale2017, 9 (46), 18246–18257. [PubMed: 28726968]

(46). Currie S; Hoggard N; Craven IJ; Hadjivassiliou M; Wilkinson IDUnderstanding MRI: basic MR physics for physicians. Postgrad. Med. J2013, 89 (1050), 209. [PubMed: 23223777]

(47). Richardson JC; Bowtell RW; Mäder K; Melia CDPharmaceutical applications of magnetic resonance imaging (MRI). Adv. Drug Delivery Rev2005, 57 (8), 1191–209.

(48). Bakker MH; Tseng CCS; Keizer HM; Seevinck PR; Janssen HM; Van Slochteren FJ; Chamuleau SAJ; Dankers PYWMRI visualization of injectable ureidopyrimidinone hydrogelators by supramolecular contrast agent labeling. Adv. Healthcare Mater2018, 7 (11), 1701139.

(49). Caravan P; Ellison JJ; McMurry TJ; Lauffer RBGadolinium(III) chelates as MRI contrast agents: structure, dynamics, and applications. Chem. Rev1999, 99 (9), 2293–2352. [PubMed: 11749483]

(50). Fraum TJ; Ludwig DR; Bashir MR; Fowler KJGadolinium-based contrast agents: A comprehensive risk assessment. J. Magn Reson Imaging2017, 46 (2), 338–353. [PubMed: 28083913]

(51). Wei H; Bruns OT; Kaul MG; Hansen EC; Barch M; Wiśniowska A; Chen O; Chen Y; Li N; Okada S; Cordero JM; Heine M; Farrar CT; Montana DM; Adam G; Ittrich H; Jasanoff A; Nielsen P; Bawendi MGExceedingly small iron oxide nanoparticles as positive MRI contrast agents. Proc. Natl. Acad. Sci. U. S. A2017, 114 (9), 2325–2330. [PubMed: 28193901]

(52). Zhu W; Chu C; Kuddannaya S; Yuan Y; Walczak P; Singh A; Song X; Bulte JWMIn vivo imaging of composite hydrogel scaffold degradation using CEST MRI and two-Color NIR imaging. Adv. Funct. Mater2019, 29 (36), 1903753. [PubMed: 32190034]

(53). Shazeeb MS; Corazzini R; Konowicz PA; Fogle R; Bangari DS; Johnson J; Ying X; Dhal PKAssessment of in vivo degradation profiles of hyaluronic acid hydrogels using temporal evolution of chemical exchange saturation transfer (CEST) MRI. Biomaterials2018, 178, 326–338. [PubMed: 29861090]

(54). Frangioni JVIn vivo near-infrared fluorescence imaging. Curr. Opin. Chem. Biol2003, 7 (5), 626–634. [PubMed: 14580568]

(55). Rao J; Dragulescu-Andrasi A; Yao HFluorescence imaging in vivo: recent advances. Curr. Opin. Biotechnol2007, 18 (1), 17–25. [PubMed: 17234399]

(56). Bouché M; Hsu JC; Dong YC; Kim J; Taing K; Cormode DPRecent advances in molecular imaging with gold nanoparticles. Bioconjugate Chem. 2020, 31 (2), 303–314.

(57). Ballou B; Ernst LA; Waggoner ASFluorescence imaging of tumors in vivo. Curr. Med. Chem2005, 12 (7), 795–805. [PubMed: 15853712]

(58). Hong G; Zou Y; Antaris AL; Diao S; Wu D; Cheng K; Zhang X; Chen C; Liu B; He Y; Wu JZ; Yuan J; Zhang B; Tao Z; Fukunaga C; Dai HUltrafast fluorescence imaging in vivo with conjugated polymer fluorophores in the second near-infrared window. Nat. Commun2014, 5 (1), 4206. [PubMed: 24947309]

(59). Koide Y; Urano Y; Hanaoka K; Piao W; Kusakabe M; Saito N; Terai T; Okabe T; Nagano TDevelopment of NIR fluorescent dyes based on Si-rhodamine for in vivo imaging. J. Am. Chem. Soc2012, 134 (11), 5029–5031. [PubMed: 22390359]

(60). Larson DR; Zipfel WR; Williams RM; Clark SW; Bruchez MP; Wise FW; Webb WWWater-soluble quantum dots for multiphoton fluorescence imaging in vivo. Science2003, 300 (5624), 1434–1436. [PubMed: 12775841]

(61). Dong Y; Jin G; Ji C; He R; Lin M; Zhao X; Li A; Lu TJ; Xu FNon-invasive tracking of hydrogel degradation using upconversion nanoparticles. Acta Biomater. 2017, 55, 410–419. [PubMed: 28428038]

(62). Belali S; Emandi G; Cafolla AA; O'Connell B; Haffner B; Möbius ME; Karimi A; Senge MOWater-soluble, neutral 3,5-diformyl-BODIPY with extended fluorescence lifetime in a self-healable chitosan hydrogel. Photochem. Photobiol. Sci2017, 16 (11), 1700–1708. [PubMed: 29039867]

(63). Patrick PS; Bear JC; Fitzke HE; Zaw-Thin M; Parkin IP; Lythgoe MF; Kalber TL; Stuckey DJRadio-metal crosslinking of alginate hydrogels for non-invasive in vivo imaging. Biomaterials2020, 243, 119930. [PubMed: 32171101]

(64). Huang W-C; Ali F; Zhao J; Rhee K; Mou C; Bettinger CJUltrasound-mediated self-healing hydrogels based on tunable metal-organic bonding. Biomacromolecules2017, 18 (4), 1162–1171. [PubMed: 28245355]

(65). Guo B; Ma PXSynthetic biodegradable functional polymers for tissue engineering: a brief review. Sci. China: Chem2014, 57 (4), 490–500. [PubMed: 25729390]

(66). Maitra JK; Shukla VKCross-linking in Hydrogels - A review. American J. Poly Sci2014, 4 (2), 25–31.

(67). Lin CC; Anseth KSPEG hydrogels for the controlled release of biomolecules in regenerative medicine. Pharm. Res2009, 26 (3), 631–43. [PubMed: 19089601]

(68). Chang C; Lue A; Zhang LEffects of crosslinking methods on structure and properties of cellulose/PVA hydrogels. Macromol. Chem. Phys2008, 209 (12), 1266–1273.

(69). Hassan CM; Peppas NACellular PVA hydrogels produced by freeze/thawing. J. Appl. Polym. Sci2000, 76 (14), 2075–2079.

(70). Park H; Kang S-W; Kim B-S; Mooney DJ; Lee KYShear-reversibly crosslinked alginate hydrogels for tissue engineering. Macromol. Biosci2009, 9 (9), 895–901. [PubMed: 19422012]

(71). Shi L; Ding P; Wang Y; Zhang Y; Ossipov D; Hilborn JSelf-healing polymeric hydrogel formed by metal-ligand coordination assembly: Design, fabrication, and biomedical applications. Macromol. Rapid Commun2019, 40 (7), 1800837.

(72). Dankers PYW; Harmsen MC; Brouwer LA; Van Luyn MJA; Meijer EWA modular and supramolecular approach to bioactive scaffolds for tissue engineering. Nat. Mater2005, 4 (7), 568–574. [PubMed: 15965478]

(73). Okay OSelf-healing hydrogels formed via hydrophobic interactions. In Supramolecular Polymer Networks and Gels; Seiffert S, Ed.; Springer International Publishing: Cham, Switzerland, 2015; pp 101–142.

(74). Rodell CB; Mealy JE; Burdick JASupramolecular guest-gost interactions for the preparation of biomedical materials. Bioconjugate Chem. 2015, 26 (12), 2279–89.

(75). Uman S; Dhand A; Burdick JARecent advances in shear-thinning and self-healing hydrogels for biomedical applications. J. Appl. Polym. Sci2020, 137 (25), 48668.

(76). Bakker MH; Lee CC; Meijer EW; Dankers PYW; Albertazzi LMulticomponent supramolecular polymers as a modular platform for intracellular delivery. ACS Nano2016, 10 (2), 1845–1852. [PubMed: 26811943]

(77). Cantekin S; de Greef TFA; Palmans ARABenzene-1,3,5-tricarboxamide: a versatile ordering moiety for supramolecular chemistry. Chem. Soc. Rev2012, 41 (18), 6125–6137. [PubMed: 22773107]

(78). Sáez JA; Escuder B; Miravet JFSelective catechol-triggered supramolecular gel disassembly. Chem. Commun. (Cambridge, U. K.)2010, 46 (42), 7996–7998.

(79). Holten-Andersen N; Harrington MJ; Birkedal H; Lee BP; Messersmith PB; Lee KYC; Waite JHpH-induced metal-ligand cross-links inspired by mussel yield self-healing polymer networks with near-covalent elastic moduli. Proc. Natl. Acad. Sci. U. S. A2011, 108 (7), 2651–2655. [PubMed: 21278337]

(80). Yavvari PS; Pal S; Kumar S; Kar A; Awasthi AK; Naaz A; Srivastava A; Bajaj AInjectable, self-healing chimeric catechol-Fe(III) hydrogel for localized combination cancer therapy. ACS Biomater. Sci. Eng2017, 3 (12), 3404–3413. [PubMed: 33445379]

(81). Fullenkamp DE; He L; Barrett DG; Burghardt WR; Messersmith PBMussel-inspired histidine-based transient network metal coordination hydrogels. Macromolecules2013, 46 (3), 1167–1174. [PubMed: 23441102]

(82). Gaharwar AK; Peppas NA; Khademhosseini ANanocomposite hydrogels for biomedical applications. Biotechnol. Bioeng2014, 111 (3), 441–453. [PubMed: 24264728]

(83). Thoniyot P; Tan MJ; Karim AA; Young DJ; Loh XJNanoparticle-hydrogel composites: Concept, design, and applications of these promising, multi-functional materials. Adv. Sci2015, 2 (1–2), 1400010.

(84). Pardo-Yissar V; Gabai R; Shipway AN; Bourenko T; Willner IGold nanoparticle/hydrogel composites with solvent-switchable electronic properties. Adv. Mater. (Weinheim, Ger.)2001, 13 (17), 1320–1323.

(85). Skardal A; Zhang J; McCoard L; Oottamasathien S; Prestwich GDDynamically crosslinked gold nanoparticle - hyaluronan hydrogels. Adv. Mater. (Weinheim, Ger.)2010, 22 (42), 4736–4740.

(86). Dasgupta A; Mondal JH; Das DPeptide hydrogels. RSC Adv. 2013, 3 (24), 9117–9149.

(87). Adams DJ; Topham PDPeptide conjugate hydrogelators. Soft Matter2010, 6 (16), 3707–3721.

(88). Kočar V; BožičAbram S; Doles T; Bašić N; Gradišar H; Pisanski T; Jerala RTOPOFOLD, the designed modular biomolecular folds: polypeptide-based molecular origami nanostructures following the footsteps of DNA. WIRES Nanomed. Nanobi2015, 7 (2), 218–237.

(89). Burdick JA; Prestwich GDHyaluronic acid hydrogels for biomedical applications. Adv. Mater2011, 23 (12), H41–56. [PubMed: 21394792]

(90). Lim KS; Galarraga JH; Cui X; Lindberg GCJ; Burdick JA; Woodfield TBFFundamentals and applications of photo-cross-linking in bioprinting. Chem. Rev. (Washington, DC, U. S.)2020, 120, 10662.

(91). Kloxin AM; Kloxin CJ; Bowman CN; Anseth KSMechanical properties of cellularly responsive hydrogels and their experimental determination. Adv. Mater2010, 22 (31), 3484–94. [PubMed: 20473984]

(92). Bowman CN; Kloxin CJToward an enhanced understanding and implementation of photopolymerization reactions. AIChE J. 2008, 54 (11), 2775–2795.

(93). Ifkovits JL; Burdick JAReview: photopolymerizable and degradable biomaterials for tissue engineering applications. Tissue Eng. 2007, 13 (10), 2369–85. [PubMed: 17658993]

(94). Williams CG; Malik AN; Kim TK; Manson PN; Elisseeff JHVariable cytocompatibility of six cell lines with photoinitiators used for polymerizing hydrogels and cell encapsulation. Biomaterials2005, 26 (11), 1211–1218. [PubMed: 15475050]

(95). Cramer NB; Bowman CNKinetics of thiol-ene and thiol-acrylate photopolymerizations with real-time fourier transform infrared. J. Polym. Sci., Part A: Polym. Chem2001, 39 (19), 3311–3319.

(96). Anderson SB; Lin CC; Kuntzler DV; Anseth KSThe performance of human mesenchymal stem cells encapsulated in cell-degradable polymer-peptide hydrogels. Biomaterials2011, 32 (14), 3564–74. [PubMed: 21334063]

(97). Gramlich WM; Kim IL; Burdick JASynthesis and orthogonal photopatterning of hyaluronic acid hydrogels with thiol-norbornene chemistry. Biomaterials2013, 34 (38), 9803–11. [PubMed: 24060422]

(98). Aimetti AA; Machen AJ; Anseth KSPoly(ethylene glycol) hydrogels formed by thiol-ene photopolymerization for enzyme-responsive protein delivery. Biomaterials2009, 30 (30), 6048–6054. [PubMed: 19674784]

(99). Nguyen QV; Huynh DP; Park JH; Lee DSInjectable polymeric hydrogels for the delivery of therapeutic agents: A review. Eur. Polym. J2015, 72, 602–619.

(100). Elbert DL; Pratt AB; Lutolf MP; Halstenberg S; Hubbell JAProtein delivery from materials formed by self-selective conjugate addition reactions. J. Controlled Release2001, 76 (1), 11–25.

(101). Peattie RA; Rieke ER; Hewett EM; Fisher RJ; Shu XZ; Prestwich GDDual growth factor-induced angiogenesis in vivo using hyaluronan hydrogel implants. Biomaterials2006, 27 (9), 1868–1875. [PubMed: 16246413]

(102). Lutolf MP; Raeber GP; Zisch AH; Tirelli N; Hubbell JACell-responsive synthetic hydrogels. Adv. Mater. (Weinheim, Ger.)2003, 15 (11), 888–892.

(103). Hiemstra C; van der Aa LJ; Zhong Z; Dijkstra PJ; Feijen JRapidly in situ-forming degradable hydrogels from dextran thiols through Michael addition. Biomacromolecules2007, 8 (5), 1548–1556. [PubMed: 17425366]

(104). Marklein RA; Burdick JASpatially controlled hydrogel mechanics to modulate stem cell interactions. Soft Matter2010, 6 (1), 136–143.

(105). Yang X; Sun Y; Kootala S; Hilborn J; Heerschap A; Ossipov DInjectable hyaluronic acid hydrogel for 19F magnetic resonance imaging. Carbohydr. Polym2014, 110, 95–9. [PubMed: 24906733]

(106). Moreira Teixeira LS; Feijen J; van Blitterswijk CA; Dijkstra PJ; Karperien MEnzyme-catalyzed crosslinkable hydrogels: emerging strategies for tissue engineering. Biomaterials2012, 33 (5), 1281–90. [PubMed: 22118821]

(107). Ranga A; Lutolf MP; Hilborn J; Ossipov DAHyaluronic acid hydrogels formed in situ by transglutaminase-catalyzed reaction. Biomacromolecules2016, 17 (5), 1553–1560. [PubMed: 27014785]

(108). Bae JW; Choi JH; Lee Y; Park KDHorseradish peroxidase-catalysed in situ-forming hydrogels for tissue-engineering applications. J. Tissue Eng. Regener. Med2015, 9 (11), 1225–32.

(109). Chen T; Embree HD; Brown EM; Taylor MM; Payne GFEnzyme-catalyzed gel formation of gelatin and chitosan: potential for in situ applications. Biomaterials2003, 24 (17), 2831–2841. [PubMed: 12742721]

(110). Lee D; Heo DN; Nah HR; Lee SJ; Ko W-K; Lee JS; Moon H-J; Bang JB; Hwang Y-S; Reis RL; Kwon IKInjectable hydrogel composite containing modified gold nanoparticles: implication in bone tissue regeneration. Int. J. Nanomed2018, 13, 7019–7031.

(111). Jin Y; Yu C; Denman RJ; Zhang WRecent advances in dynamic covalent chemistry. Chem. Soc. Rev2013, 42 (16), 6634–6654. [PubMed: 23749182]

(112). Uman S; Wang LL; Thorn SL; Liu Z; Duncan JS; Sinusas AJ; Burdick JAImaging of injectable hydrogels delivered into myocardium with SPECT/CT. Adv. Healthcare Mater2020, 9 (14), 2000294.

(113). Lin F; Yu J; Tang W; Zheng J; Defante A; Guo K; Wesdemiotis C; Becker MLPeptide-functionalized oxime hydrogels with tunable mechanical properties and gelation behavior. Biomacromolecules2013, 14 (10), 3749–3758. [PubMed: 24050500]

(114). Grover GN; Braden RL; Christman KLOxime cross-linked injectable hydrogels for catheter delivery. Adv. Mater2013, 25 (21), 2937–42. [PubMed: 23495015]

(115). Sun Y; Huang YDisulfide-crosslinked albumin hydrogels. J. Mater. Chem. B2016, 4 (16), 2768–2775. [PubMed: 32263341]

(116). Choh S-Y; Cross D; Wang CFacile synthesis and characterization of disulfide-cross-linked hyaluronic acid hydrogels for protein delivery and cell encapsulation. Biomacromolecules2011, 12 (4), 1126–1136. [PubMed: 21384907]

(117). Han X; Huang J; To AKW; Lai JHC; Xiao P; Wu EX; Xu J; Chan KWYCEST MRI detectable liposomal hydrogels for multiparametric monitoring in the brain at 3T. Theranostics2020, 10 (5), 2215–2228. [PubMed: 32089739]

(118). Lock LL; Li Y; Mao X; Chen H; Staedtke V; Bai R; Ma W; Lin R; Li Y; Liu G; Cui HOne-component supramolecular filament hydrogels as theranostic label-free magnetic resonance imaging agents. ACS Nano2017, 11 (1), 797–805. [PubMed: 28075559]

(119). Dorsey SM; Haris M; Singh A; Witschey WRT; Rodell CB; Kogan F; Reddy R; Burdick JAVisualization of injectable hydrogels using chemical exchange saturation transfer MRI. ACS Biomater. Sci. Eng2015, 1 (4), 227–237. [PubMed: 33435047]

(120). Xu H-X; Tan Y; Wang D; Wang X-L; An W-L; Xu P-P; Xu S; Wang Y-ZAutofluorescence of hydrogels without a fluorophore. Soft Matter2019, 15 (17), 3588–3594. [PubMed: 30964145]

(121). Tsou Y-H; Zhang X-Q; Bai X; Zhu H; Li Z; Liu Y; Shi J; Xu XDopant-free hydrogels with intrinsic photoluminescence and biodegradable properties. Adv. Funct. Mater2018, 28 (34), 1802607.

(122). Ma X; Sun X; Hargrove D; Chen J; Song D; Dong Q; Lu X; Fan T-H; Fu Y; Lei YA biocompatible and biodegradable protein hydrogel with green and red autofluorescence: preparation, characterization and in vivo biodegradation tracking and modeling. Sci. Rep2016, 6 (1), 19370. [PubMed: 26813916]

(123). Wu Y; Wang H; Gao F; Xu Z; Dai F; Liu WAn injectable supramolecular polymer nanocomposite hydrogel for prevention of breast cancer recurrence with theranostic and mammoplastic functions. Adv. Funct. Mater2018, 28 (21), 1801000.

(124). Keshavarz M; Moloudi K; Paydar R; Abed Z; Beik J; Ghaznavi H; Shakeri-Zadeh AAlginate hydrogel co-loaded with cisplatin and gold nanoparticles for computed tomography image-guided chemotherapy. J. Biomater. Appl2018, 33 (2), 161–169. [PubMed: 29933708]

(125). Celikkin N; Mastrogiacomo S; Walboomers XF; Swieszkowski WEnhancing X-ray attenuation of 3D printed gelatin methacrylate (GelMA) hydrogels utilizing gold nanoparticles for bone tissue engineering applications. Polymers (Basel, Switz.)2019, 11 (2), 367.

(126). Wang C; Wang X; Dong K; Luo J; Zhang Q; Cheng YInjectable and responsively degradable hydrogel for personalized photothermal therapy. Biomaterials2016, 104, 129–137. [PubMed: 27449949]

(127). Zhang Y; Gao H; Wang H; Xu Z; Chen X; Liu B; Shi Y; Lu Y; Wen L; Li Y; Li Z; Men Y; Feng X; Liu WRadiopaque highly stiff and tough shape memory hydrogel microcoils for permanent embolization of arteries. Adv. Funct. Mater2018, 28 (9), 1705962.

(128). Coutu JM; Fatimi A; Berrahmoune S; Soulez G; Lerouge SA new radiopaque embolizing agent for the treatment of endoleaks after endovascular repair: influence of contrast agent on chitosan thermogel properties. J. Biomed. Mater. Res., Part B2013, 101B (1), 153–161.

(129). Kim JI; Lee BS; Chun C; Cho JK; Kim SY; Song SCLong-term theranostic hydrogel system for solid tumors. Biomaterials2012, 33 (7), 2251–9. [PubMed: 22189146]

(130). Chen B; Xing J; Li M; Liu Y; Ji MDOX@Ferumoxytol-Medical Chitosan as magnetic hydrogel therapeutic system for effective magnetic hyperthermia and chemotherapy in vitro. Colloids Surf., B2020, 190, 110896.

(131). Carvalho A; Gallo J; Pereira DM; Valentão P; Andrade PB; Hilliou L; Ferreira PMT; Bañobre-López M; Martins JAMagnetic Dehydrodipeptide-Based Self-Assembled Hydrogels for Theragnostic Applications. Nanomaterials2019, 9 (4), 541.

(132). Wang L; Li B; Xu F; Li Y; Xu Z; Wei D; Feng Y; Wang Y; Jia D; Zhou YVisual in vivo degradation of injectable hydrogel by real-time and non-invasive tracking using carbon nanodots as fluorescent indicator. Biomaterials2017, 145, 192–206. [PubMed: 28869865]

(133). Jin H; Zhao G; Hu J; Ren Q; Yang K; Wan C; Huang A; Li P; Feng JP; Chen J; Zou ZMelittin-containing hybrid peptide hydrogels for enhanced photothermal therapy of glioblastoma. ACS Appl. Mater. Interfaces2017, 9 (31), 25755–25766. [PubMed: 28714303]

(134). Kim JH; Lim SY; Nam DH; Ryu J; Ku SH; Park CBSelf-assembled, photoluminescent peptide hydrogel as a versatile platform for enzyme-based optical biosensors. Biosens. Bioelectron2011, 26 (5), 1860–5. [PubMed: 20171868]

(135). Li P; Chen W; Yan Y; Chen B; Wang Y; Huang XLaser-triggered injectable gelatin hydrogels system for combinatorial upconversion fluorescence imaging and antitumor chemophotothermal therapy. ACS Applied Bio Materials2019, 2 (9), 3722–3729.

(136). He W; Li P; Zhu Y; Liu M; Huang X; Qi HAn injectable silk fibroin nanofiber hydrogel hybrid system for tumor upconversion luminescence imaging and photothermal therapy. New J. Chem2019, 43 (5), 2213–2219.

(137). Cheng M; Peng W; Hua P; Chen Z; Sheng J; Yang J; Wu YIn situ formation of pH-responsive Prussian blue for photoacoustic imaging and photothermal therapy of cancer. RSC Adv. 2017, 7 (30), 18270–18276.

(138). Wu H; Song L; Chen L; Huang Y; Wu Y; Zang F; An Y; Lyu H; Ma M; Chen J; Gu N; Zhang YInjectable thermosensitive magnetic nanoemulsion hydrogel for multimodal-imaging-guided accurate thermoablative cancer therapy. Nanoscale2017, 9 (42), 16175–16182. [PubMed: 28770920]

(139). Bermejo-Velasco D; Dou W; Heerschap A; Ossipov D; Hilborn JInjectable hyaluronic acid hydrogels with the capacity for magnetic resonance imaging. Carbohydr. Polym2018, 197, 641–648. [PubMed: 30007657]

(140). Courant T; Roullin VG; Cadiou C; Callewaert M; Andry MC; Portefaix C; Hoeffel C; de Goltstein MC; Port M; Laurent S; Elst LV; Muller R; Molinari M; Chuburu FHydrogels incorporating GdDOTA: towards highly efficient dual T1/T2MRI contrast agents. Angew. Chem., Int. Ed2012, 51 (36), 9119–9122.

(141). Heo YJ; Shibata H; Okitsu T; Kawanishi T; Takeuchi SLong-term in vivo glucose monitoring using fluorescent hydrogel fibers. Proc. Natl. Acad. Sci. U. S. A2011, 108 (33), 13399–13403. [PubMed: 21808049]

(142). Dong X; Wei C; Liu T; Lv F; Qian ZReal-time fluorescence tracking of protoporphyrin incorporated thermosensitive hydrogel and its drug release in vivo. ACS Appl. Mater. Interfaces2016, 8 (8), 5104–5113. [PubMed: 26848506]

(143). Oyen E; Martin C; Caveliers V; Madder A; Van Mele B; Hoogenboom R; Hernot S; Ballet SIn vivo imaging of the stability and sustained cargo release of an injectable amphipathic peptide-based hydrogel. Biomacromolecules2017, 18 (3), 994–1001. [PubMed: 28192660]

(144). Laurén P; Lou Y-R; Raki M; Urtti A; Bergström K; Yliperttula MTechnetium-99m-labeled nanofibrillar cellulose hydrogel for in vivo drug release. Eur. J. Pharm. Sci2014, 65, 79–88. [PubMed: 25245005]

(145). op ‘t Veld RC; Joosten L; van den Boomen OI; Boerman OC; Kouwer P; Middelkoop E; Rowan AE; Jansen JA; Walboomers XF; Wagener FADTGMonitoring 111In-labelled polyisocyanopeptide (PIC) hydrogel wound dressings in full-thickness wounds. Biomater. Sci2019, 7 (7), 3041–3050. [PubMed: 31115398]

(146). Chen X; Zhang J; Wu K; Wu X; Tang J; Cui S; Cao D; Liu R; Peng C; Yu L; Ding JVisualizing the in vivo evolution of an injectable and thermosensitive hydrogel using tri-modal bioimaging. Small Methods2020, 4 (9), 2000310.

(147). Kulkarni K; Hung J; Fulcher AJ; Chan AHP; Hong A; Forsythe JS; Aguilar M-I; Wise SG; Del Borgo MPβ3-tripeptides coassemble into fluorescent hydrogels for serial monitoring in vivo. ACS Biomater. Sci. Eng2018, 4 (11), 3843–3847. [PubMed: 33429591]

(148). Zhang M; Wang Z; Huang P; Jiang G; Xu C; Zhang W; Guo R; Li W; Zhang XReal-time and noninvasive tracking of injectable hydrogel degradation using functionalized AIE nanoparticles. Nanophotonics2020, 9 (7), 2063.

(149). Li Q-F; Chu S; Li E; Li M; Wang J-T; Wang ZLanthanide-based hydrogels with adjustable luminescent properties synthesized by thiol-Michael addition. Dyes Pigm. 2020, 174, 108091.

(150). Szulc DA; Cheng H-LMOne-step labeling of collagen hydrogels with polydopamine and manganese porphyrin for noninvasive scaffold tracking on magnetic resonance imaging. Macromol. Biosci2019, 19 (4), 1800330.

(151). Al-Mahamad LLGGold nanoparticles driven self-assembling hydrogel via Host-Guest system. J. Mol. Struct2020, 1200, 127063.

(152). Bouché M; Pühringer M; Iturmendi A; Amirshaghaghi A; Tsourkas A; Teasdale I; Cormode DPActivatable hybrid polyphosphazene-AuNP nanoprobe for ROS detection by bimodal PA/CT imaging. ACS Appl. Mater. Interfaces2019, 11 (32), 28648–28656. [PubMed: 31321973]

(153). Kim J; Bar-Ness D; Si-Mohamed S; Coulon P; Blevis I; Douek P; Cormode DPAssessment of candidate elements for development of spectral photon-counting CT specific contrast agents. Sci. Rep2018, 8 (1), 12119. [PubMed: 30108247]

(154). Dong YC; Hajfathalian M; Maidment PSN; Hsu JC; Naha PC; Si-Mohamed S; Breuilly M; Kim J; Chhour P; Douek P; Litt HI; Cormode DPEffect of gold nanoparticle size on their properties as contrast agents for computed tomography. Sci. Rep2019, 9 (1), 14912. [PubMed: 31624285]

(155). Hotze EM; Phenrat T; Lowry GVNanoparticle Aggregation: Challenges to Understanding Transport and Reactivity in the Environment. J. Environ. Qual2010, 39 (6), 1909–1924. [PubMed: 21284288]

(156). Manson J; Kumar D; Meenan BJ; Dixon DPolyethylene glycol functionalized gold nanoparticles: the influence of capping density on stability in various media. Gold Bull. 2011, 44 (2), 99–105.

(157). Jalani G; Naccache R; Rosenzweig DH; Lerouge S; Haglund L; Vetrone F; Cerruti MReal-time, non-invasive monitoring of hydrogel degradation using LiYF4:Yb3+/Tm3+ NIR-to-NIR upconverting nanoparticles. Nanoscale2015, 7 (26), 11255–11262. [PubMed: 26067274]

(158). Kim JI; Chun C; Kim B; Hong JM; Cho J-K; Lee SH; Song S-CThermosensitive/magnetic poly(organophosphazene) hydrogel as a long-term magnetic resonance contrast platform. Biomaterials2012, 33 (1), 218–224. [PubMed: 21975461]

(159). Carvalho A; Gallo J; Pereira DM; Valentão P; Andrade PB; Hilliou L; Ferreira PMT; Bañobre-López M; Martins JAMagnetic Dehydrodipeptide-Based Self-Assembled Hydrogels for Theragnostic Applications. Nanomaterials2019, 9 (4), 541.

(160). Wang W; Liu J; Li C; Zhang J; Liu J; Dong A; Kong DReal-time and non-invasive fluorescence tracking of in vivo degradation of the thermosensitive PEGlyated polyester hydrogel. J. Mater. Chem. B2014, 2 (26), 4185–4192. [PubMed: 32261752]

(161). Wang H-H; Fu Z-G; Li W; Li Y-X; Zhao L-S; Wen L; Zhang J-J; Wen NThe synthesis and application of nano doxorubicin- indocyanine green matrix metalloproteinase-responsive hydrogel in chemophototherapy for head and neck squamous cell carcinoma. Int. J. Nanomed2019, 14, 623–638.

(162). Fisher DR; Fidel J; Maitz CADirect interstitial treatment of solid tumors using an injectable yttrium-90-polymer composite. Cancer Biother.Radiopharm2020, 35 (1), 1–9. [PubMed: 31621382]

(163). Shanks HR; Milani AH; Lu D; Saunders BR; Carney L; Adlam DJ; Hoyland JA; Blount C; Dickinson MCore-shell-shell nanoparticles for NIR fluorescence imaging and NRET swelling reporting of injectable or implantable gels. Biomacromolecules2019, 20 (7), 2694–2702. [PubMed: 31185170]

(164). Kim MG; Kang TW; Park JY; Park SH; Ji YB; Ju HJ; Kwon DY; Kim YS; Kim SW; Lee B; Choi HS; Lee HB; Kim JH; Lee BY; Min BH; Kim MSAn injectable cationic hydrogel electrostatically interacted with BMP2 to enhance in vivo osteogenic differentiation of human turbinate mesenchymal stem cells. Mater. Sci. Eng., C2019, 103, 109853.

(165). Li Q; Feng Z; Song H; Zhang J; Dong A; Kong D; Wang W; Huang P19F magnetic resonance imaging enabled real-time, non-invasive and precise localization and quantification of the degradation rate of hydrogel scaffolds in vivo. Biomater. Sci2020, 8 (12), 3301–3309. [PubMed: 32356855]

(166). Samuel R; Girard E; Chagnon G; Dejean S; Favier D; Coudane J; Nottelet BRadiopaque poly(ε-caprolactone) as additive for X-ray imaging of temporary implantable medical devices. RSC Adv. 2015, 5 (102), 84125–84133.

(167). Banerjee SL; Hoskins R; Swift T; Rimmer S; Singha NKA self-healable fluorescence active hydrogel based on ionic block copolymers prepared via ring opening polymerization and xanthate mediated RAFT polymerization. Polym. Chem2018, 9 (10), 1190–1205.

(168). Dzhonova D; Olariu R; Leckenby J; Dhayani A; Vemula PK; Prost JC; Banz Y; Taddeo A; Rieben RLocal release of tacrolimus from hydrogel-based drug delivery system is controlled by inflammatory enzymes in vivo and can be monitored non-invasively using in vivo imaging. PLoS One2018, 13 (8), No. e0203409. [PubMed: 30161258]

(169). Lei K; Shen W; Cao L; Yu L; Ding JAn injectable thermogel with high radiopacity. Chem. Commun. (Cambridge, U. K.)2015, 51 (28), 6080–6083.

(170). Huang P; Song H; Zhang Y; Liu J; Cheng Z; Liang XJ; Wang W; Kong D; Liu JFRET-enabled monitoring of the thermosensitive nanoscale assembly of polymeric micelles into macroscale hydrogel and sequential cognate micelles release. Biomaterials2017, 145, 81–91. [PubMed: 28858720]

(171). Lei K; Chen Y; Wang J; Peng X; Yu L; Ding JNoninvasive monitoring of in vivo degradation of a radiopaque thermoreversible hydrogel and its efficacy in preventing postoperative adhesions. Acta Biomater. 2017, 55, 396–409. [PubMed: 28363786]

(172). Patterson JChapter 10: Imaging hydrogel implants in situ. In Biomedical Hydrogels; Rimmer S, Ed.; Woodhead Publishing, 2011; pp 228–255.

(173). Saremi F; Achenbach SCoronary Plaque Characterization Using CT. AJR, Am. J. Roentgenol2015, 204 (3), W249–W260. [PubMed: 25714309]

(174). Beinfeld MT; Wittenberg E; Gazelle GSCost-effectiveness of Whole-Body CT Screening. Radiology2005, 234 (2), 415–422. [PubMed: 15670999]

(175). Grover VPB; Tognarelli JM; Crossey MME; Cox IJ; Taylor-Robinson SD; McPhail MJWMagnetic resonance imaging: principles and techniques: lessons for clinicians. J. Clin. Exp. Hepatol2015, 5 (3), 246–255. [PubMed: 26628842]

(176). Meredith WJ; Massey JBThe production of X-rays. In Fundamental Physics of Radiology, 3rd ed.; Meredith WJ, Massey JB, Eds.; Butterworth-Heinemann: Oxford, U.K., 1977; pp 44–56.

(177). Percuoco RChapter 1: Plain radiographic imaging. In Clinical Imaging, 3rd ed.; Marchiori DM, Ed.; Mosby: Saint Louis, MO, 2014; pp 1–43.

(178). Ying X; Barlow NJ; Feuston MHChapter 75: Micro-CT and volumetric imaging in developmental toxicology. In Reproductive and Developmental Toxicology; Gupta RC, Ed.; Academic Press: San Diego, CA, 2011; pp 983–1000.

(179). Goldman LWPrinciples of CT and CT technology. J. Nucl. Med. Technol2007, 35 (3), 115–28 quiz 129–30.. [PubMed: 17823453]

(180). Jensen EA; Mong DA; Biko DM; Maschhoff KL; Kirpalani HImaging: radiography, lung ultrasound, and other imaging modalities. In Assisted Ventilation of the Neonate, 6th ed.; Goldsmith JP, Karotkin EH, Keszler M, Suresh GK, Eds.; Elsevier: Amsterdam, The Netherlands, 2017; pp 67–79.

(181). Paulson EK; Sheafor DH; Enterline DS; McAdams HP; Yoshizumi TTCT fluoroscopy–guided interventional procedures: techniques and radiation dose to radiologists. Radiology2001, 220 (1), 161–7. [PubMed: 11425990]

(182). Si-Mohamed S; Tatard-Leitman V; Laugerette A; Sigovan M; Pfeiffer D; Rummeny EJ; Coulon P; Yagil Y; Douek P; Boussel L; Noël PBSpectral Photon-Counting Computed Tomography

(SPCCT): in-vivo single-acquisition multi-phase liver imaging with a dual contrast agent protocol. Sci. Rep2019, 9 (1), 8458. [PubMed: 31186467]

(183). Si-Mohamed S; Thivolet A; Bonnot PE; Bar-Ness D; Kepenekian V; Cormode DP; Douek P; Rousset PImproved peritoneal cavity and abdominal organ imaging using a biphasic contrast agent protocol and spectral photon counting computed tomography K-edge imaging. Invest. Radiol2018, 53 (10), 629–639. [PubMed: 29794948]

(184). Sabel MSChapter 2: Principles of breast cancer screening. In Essentials of Breast Surgery; Sabel MS, Ed.; Mosby: Philadelphia, PA, 2009; pp 19–40.

(185). McKetty MHThe AAPM/RSNA physics tutorial for residents. X-ray attenuation. Radiographics1998, 18 (1), 151–163. [PubMed: 9460114]

(186). Momose A; Takeda T; Itai Y; Hirano KPhase-contrast X-ray computed tomography for observing biological soft tissues. Nat. Med. (N. Y., NY, U. S.)1996, 2 (4), 473–475.

(187). Broder JChapter 9: Imaging of nontraumatic abdominal conditions. In Diagnostic Imaging for the Emergency Physician; Broder J, Ed.; W. B. Saunders: Saint Louis, MO, 2011; pp 445–577.

(188). Lusic H; Grinstaff MWX-ray-computed tomography contrast agents. Chem. Rev. (Washington, DC, U. S.)2013, 113 (3), 1641–1666.

(189). Atluri PS; Gannavarapu BS; Timmerman RD; Garant A; Hannan R; Folkert MR; Desai NBAddition of iodinated contrast to rectal hydrogel spacer to facilitate MRI-independent target delineation and treatment planning for prostate cancer. Pract. Radiat. Oncol2019, 9 (6), e528–e533. [PubMed: 31173917]

(190). Bair RJ; Bair E; Viswanathan ANA radiopaque polymer hydrogel used as a fiducial marker in gynecologic-cancer patients receiving brachytherapy. Brachytherapy2015, 14 (6), 876–880. [PubMed: 26481393]

(191). Naha PC; Chhour P; Cormode DPSystematic in vitro toxicological screening of gold nanoparticles designed for nanomedicine applications. Toxicol. In Vitro2015, 29 (7), 1445–53. [PubMed: 26031843]

(192). de Souza Lawrence L; Ford E; Gilbert C; Yarmus L; Meneshian A; Feller-Kopman D; Hales RNovel applications of an injectable radiopaque hydrogel tissue marker for management of thoracic malignancies. Chest2013, 143 (6), 1635–1641. [PubMed: 23287908]

(193). Bair RJ; Bair E; Viswanathan ANA radiopaque polymer hydrogel used as a fiducial marker in gynecologic-cancer patients receiving brachytherapy. Brachytherapy2015, 14 (6), 876–80. [PubMed: 26481393]

(194). Struik GM; Hoekstra N; Klem TM; Ghandi A; Verduijn GM; Swaak-Kragten AT; Schoonbeek A; de Vries KC; Sattler MA; Verhoef K; Birnie E; Pignol JPInjection of radiopaque hydrogel at time of lumpectomy improves the target definition for adjuvant radiotherapy. Radiother. Oncol2019, 131, 8–13. [PubMed: 30773191]

(195). Datta S; Jana S; Das A; Chakraborty A; Chowdhury AR; Datta PBioprinting of radiopaque constructs for tissue engineering and understanding degradation behavior by use of Micro-CT. Bioact. Mater2020, 5 (3), 569–576. [PubMed: 32373763]

(196). Gibby WABasic principles of magnetic resonance imaging. Neurosurg. Clin2005, 16 (1), 1–64.

(197). Wahsner J; Gale EM; Rodríguez-Rodríguez A; Caravan PChemistry of MRI contrast agents: current challenges and new frontiers. Chem. Rev. (Washington, DC, U. S.)2019, 119 (2), 957–1057.

(198). Xiao YD; Paudel R; Liu J; Ma C; Zhang ZS; Zhou SKMRI contrast agents: Classification and application (Review). Int. J. Mol. Med2016, 38 (5), 1319–1326. [PubMed: 27666161]

(199). van Zijl PCM; Yadav NNChemical exchange saturation transfer (CEST): what is in a name and what isn't?Magn. Reson. Med2011, 65 (4), 927–948. [PubMed: 21337419]

(200). Jones KM; Pollard AC; Pagel MDClinical applications of chemical exchange saturation transfer (CEST) MRI. J. Magn Reson Imaging2018, 47 (1), 11–27. [PubMed: 28792646]

(201). Do C; Barnes JL; Tan C; Wagner BType of MRI contrast, tissue gadolinium, and fibrosis. Am. J. Physiol. Renal Physiol2014, 307 (7), F844–F855. [PubMed: 25100280]

(202). Liang Y; Bar-Shir A; Song X; Gilad AA; Walczak P; Bulte JWMLabel-free imaging of gelatin-containing hydrogel scaffolds. Biomaterials2015, 42, 144–150. [PubMed: 25542802]

(203). Jin T; Nicholls FJ; Crum WR; Ghuman H; Badylak SF; Modo MDiamagnetic chemical exchange saturation transfer (diaCEST) affords magnetic resonance imaging of extracellular matrix hydrogel implantation in a rat model of stroke. Biomaterials2017, 113, 176–190. [PubMed: 27816001]

(204). Kosaka N; Ogawa M; Choyke PL; Kobayashi HClinical implications of near-infrared fluorescence imaging in cancer. Future Oncol. 2009, 5 (9), 1501–1511. [PubMed: 19903075]

(205). Shashkova S; Leake MCSingle-molecule fluorescence microscopy review: shedding new light on old problems. Biosci. Rep2017, 37 (4), BSR20170031. [PubMed: 28694303]

(206). Haustein E; Schwille PTrends in fluorescence imaging and related techniques to unravel biological information. HFSP J. 2007, 1 (3), 169–180. [PubMed: 19404444]

(207). Debie P; Hernot SEmerging fluorescent molecular tracers to guide intra-operative surgical decision-making. Front. Pharmacol2019, 10, 510. [PubMed: 31139085]

(208). Pansare VJ; Hejazi S; Faenza WJ; Prud'homme RKReview of long-wavelength optical and NIR imaging materials: contrast agents, fluorophores, and multifunctional nano carriers. Chem. Mater2012, 24 (5), 812–827. [PubMed: 22919122]

(209). Leblond F; Davis SC; Valdés PA; Pogue BWPre-clinical whole-body fluorescence imaging: Review of instruments, methods and applications. J. Photochem. Photobiol., B2010, 98 (1), 77–94. [PubMed: 20031443]

(210). Li Y; Young DJ; Loh XJFluorescent gels: a review of synthesis, properties, applications and challenges. Mater. Chem. Front2019, 3 (8), 1489–1502.

(211). Zhao J; Li J; Zhu C; Hu F; Wu H; Man X; Li Z; Ye C; Zou D; Wang SDesign of phase-changeable and injectable alginate hydrogel for imaging-guided tumor hyperthermia and chemotherapy. ACS Appl. Mater. Interfaces2018, 10 (4), 3392–3404. [PubMed: 29313334]

(212). Jin R; Yang J; Ding P; Li C; Zhang B; Chen W; Zhao YD; Cao Y; Liu BAntitumor immunity triggered by photothermal therapy and photodynamic therapy of a 2D MoS(2) nanosheet-incorporated injectable polypeptide-engineered hydrogel combinated with chemotherapy for 4T1 breast tumor therapy. Nanotechnology2020, 31 (20), 205102. [PubMed: 32018232]

(213). Wang C; Cheng L; Liu ZUpconversion nanoparticles for photodynamic therapy and other cancer therapeutics. Theranostics2013, 3 (5), 317–330. [PubMed: 23650479]

(214). Jung IY; Kim JS; Choi BR; Lee K; Lee HHydrogel based biosensors for in vitro diagnostics of biochemicals, proteins, and genes. Adv. Healthcare Mater2017, 6 (12), 1601475.

(215). Tavakoli J; Tang YHydrogel based sensors for biomedical applications: An updated review. Polymers (Basel, Switz.)2017, 9 (8), 364.

(216). Song H; Zhang Y; Wang S; Huang K; Luo Y; Zhang W; Xu WLabel-free polygonal-plate fluorescent-hydrogel biosensor for ultrasensitive microRNA detection. Sens. Actuators, B2020, 306, 127554.

(217). Xiong H; Zheng H; Wang W; Liang J; Wen W; Zhang X; Wang SA convenient purification method for silver nanoclusters and its applications in fluorescent pH sensors for bacterial monitoring. Biosens. Bioelectron2016, 86, 164–168. [PubMed: 27371824]

(218). Zhang X; Yang S; Jiang R; Sun L; Pang S; Luo AFluorescent molecularly imprinted membranes as biosensor for the detection of target protein. Sens. Actuators, B2018, 254, 1078–1086.

(219). Jia H; Li Z; Wang X; Zheng ZFacile functionalization of a tetrahedron-like PEG macromonomer-based fluorescent hydrogel with high strength and its heavy metal ion detection. J. Mater. Chem. A2015, 3 (3), 1158–1163.

(220). Zanzonico PAn overview of nuclear imaging. In Radio-pharmaceutical Chemistry; Lewis JS, Windhorst AD, Zeglis BM, Eds.; Springer International Publishing: Cham, Switzerland, 2019; pp 101–117.

(221). Miller DL; Smith NB; Bailey MR; Czarnota GJ; Hynynen K; Makin IRSOverview of therapeutic ultrasound applications and safety considerations. J. Ultrasound Med2012, 31 (4), 623–634. [PubMed: 22441920]

(222). Whitworth M; Bricker L; Neilson JP; Dowswell TUltrasound for fetal assessment in early pregnancy. In Cochrane Database of Systematic Reviews; John Wiley & Sons, Ltd.: Chichester, U.K., 2010; p CD007058,.

(223). Parvizi D; Haas F; Peintinger F; Hubmer M; Rappl T; Koch H; Schintler M; Spendel S; Kamolz LP; Wurzer P; Tuca A; Fuchsjaeger M; Weinke RFirst experience using contrast-enhanced ultrasound to evaluate vascularisation of acellular dermal matrices after implant-based breast reconstruction. Breast J. 2014, 20 (5), 461–7. [PubMed: 25041092]

(224). Chang EHAn introduction to contrast-enhanced ultrasound for nephrologists. Nephron2018, 138 (3), 176–185. [PubMed: 29131073]

(225). Madsen HHT; Rasmussen FContrast-enhanced ultrasound in oncology. Cancer Imaging2011, 11 (1A), S167–S173. [PubMed: 22186152]

(226). Huebsch N; Kearney CJ; Zhao X; Kim J; Cezar CA; Suo Z; Mooney DJUltrasound-triggered disruption and self-healing of reversibly cross-linked hydrogels for drug delivery and enhanced chemotherapy. Proc. Natl. Acad. Sci. U. S. A2014, 111 (27), 9762–9767. [PubMed: 24961369]

(227). Xia J; Yao J; Wang LVPhotoacoustic tomography: principles and advances. Electromagn Waves (Camb)2014, 147, 1–22. [PubMed: 25642127]

(228). Beard PBiomedical photoacoustic imaging. Interface Focus2011, 1 (4), 602–631. [PubMed: 22866233]

(229). Tondera C; Hauser S; Krüger-Genge A; Jung F; Neffe AT; Lendlein A; Klopfleisch R; Steinbach J; Neuber C; Pietzsch JGelatin-based hydrogel degradation and tissue interaction in vivo: Insights from multimodal preclinical imaging in immunocompetent nude mice. Theranostics2016, 6 (12), 2114–2128. [PubMed: 27698944]

(230). Bruckman MA; Yu X; Steinmetz NFEngineering Gd-loaded nanoparticles to enhance MRI sensitivity via T(1) shortening. Nanotechnology2013, 24 (46), 462001–462001. [PubMed: 24158750]

(231). Dhingra VK; Mahajan A; Basu SEmerging clinical applications of PET based molecular imaging in oncology: the promising future potential for evolving personalized cancer care. Indian J. Radiol Imaging2015, 25 (4), 332–341. [PubMed: 26752813]

(232). Griffeth LKUse of PET/CT scanning in cancer patients: technical and practical considerations. Proc. (Bayl Univ Med. Cent)2005, 18 (4), 321–330. [PubMed: 16252023]

(233). Lee D-E; Koo H; Sun I-C; Ryu JH; Kim K; Kwon ICMultifunctional nanoparticles for multimodal imaging and theragnosis. Chem. Soc. Rev2012, 41 (7), 2656–2672. [PubMed: 22189429]

(234). Xie J; Lee S; Chen XNanoparticle-based theranostic agents. Adv. Drug Delivery Rev2010, 62 (11), 1064–1079.

(235). Mandal A; Clegg JR; Anselmo AC; Mitragotri SHydrogels in the clinic. Bioeng. Transl. Med2020, 5 (2), No. e10158–e10158. [PubMed: 32440563]

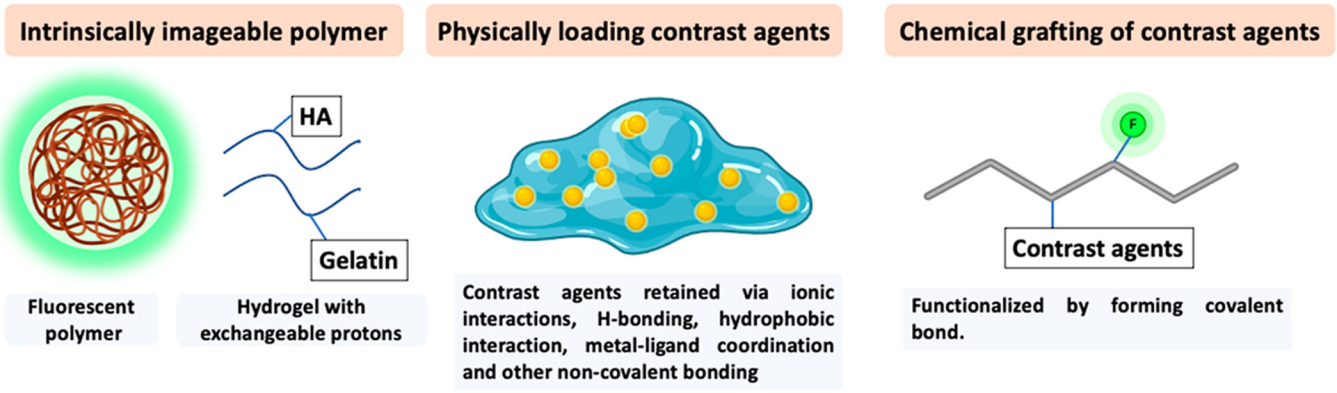

Figure 1.

Schematic of various strategies to image hydrogels. This figure was created with BioRender.com.

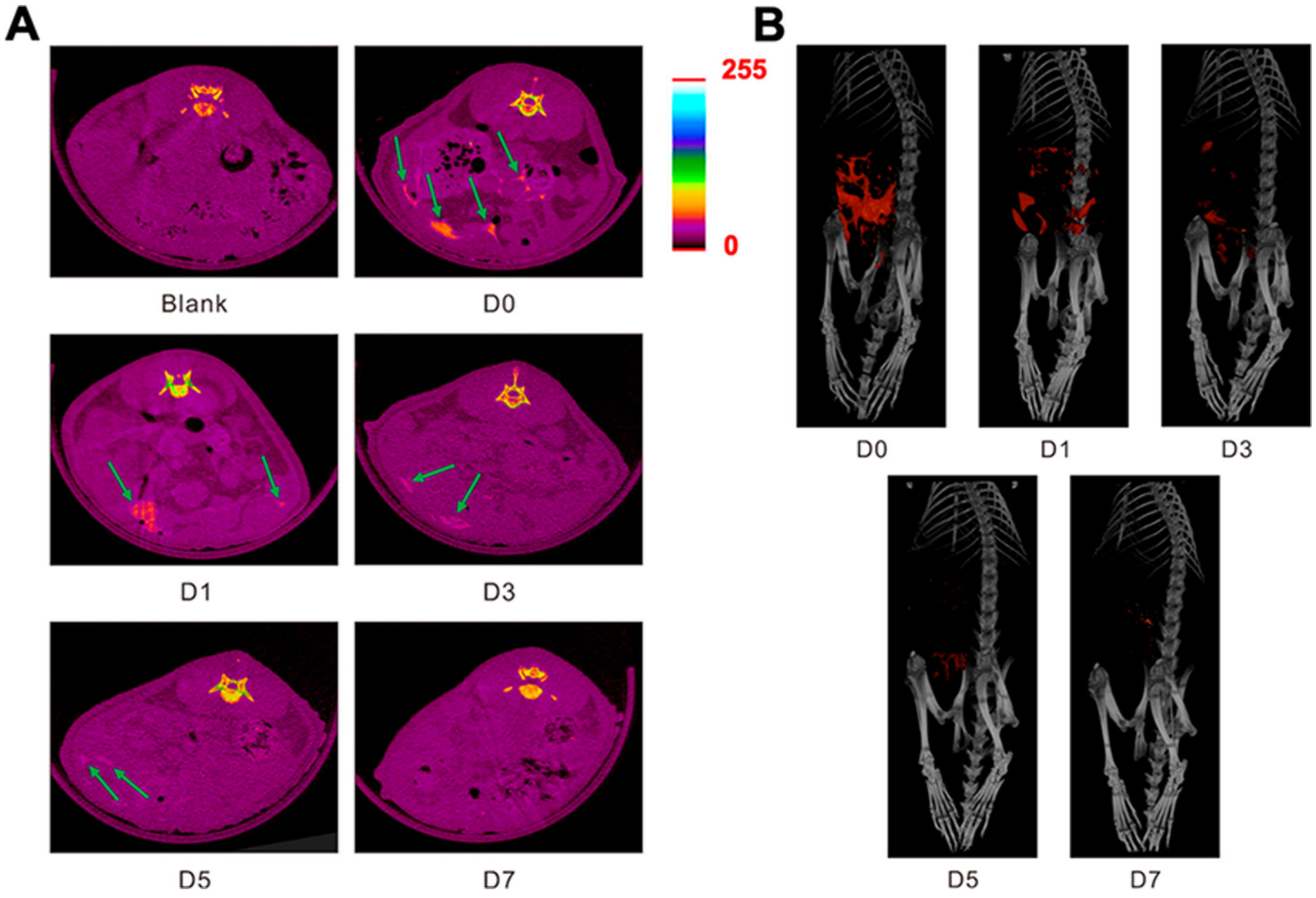

Figure 2.

(A) Transverse CT images of a rat during the week after receiving radiopaque hydrogel treatments. (B) 3D reconstructions of CT images of a rat after treatment with the radiopaque hydrogel at the indicated time points. This figure is reproduced with permission from ref 171. Copyright 2017 Elsevier.

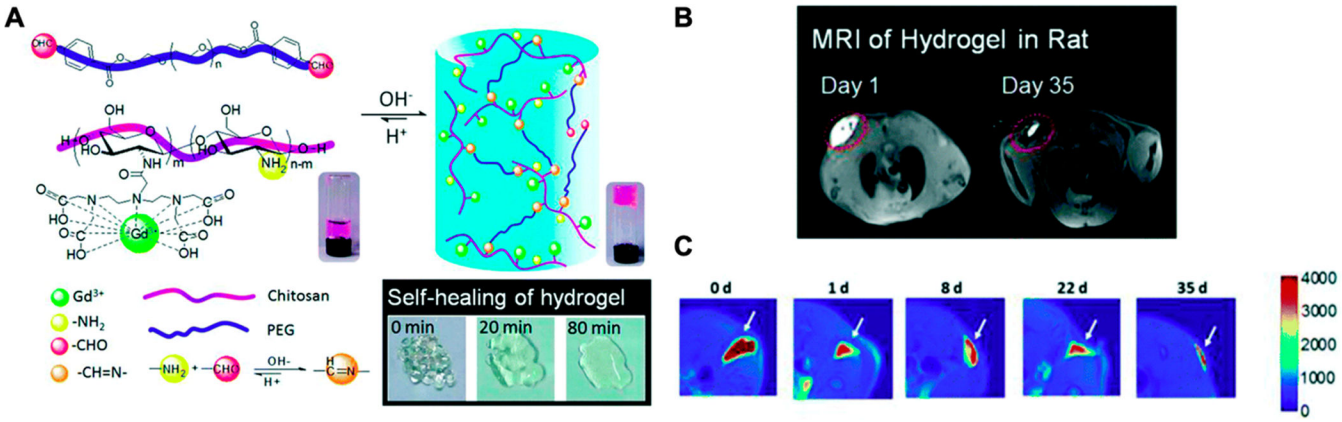

Figure 3.

(A) Illustration of the formation of the self-healing hydrogel. (B) MRI image of rat after subcutaneous injection of hydrogels. (C) Transverse cross sections of pseudocolored MR images of rat after subcutaneous injection of hydrogels at different time-points. This figure is reproduced with permission from ref 32. Copyright 2013 Royal Society of Chemistry.

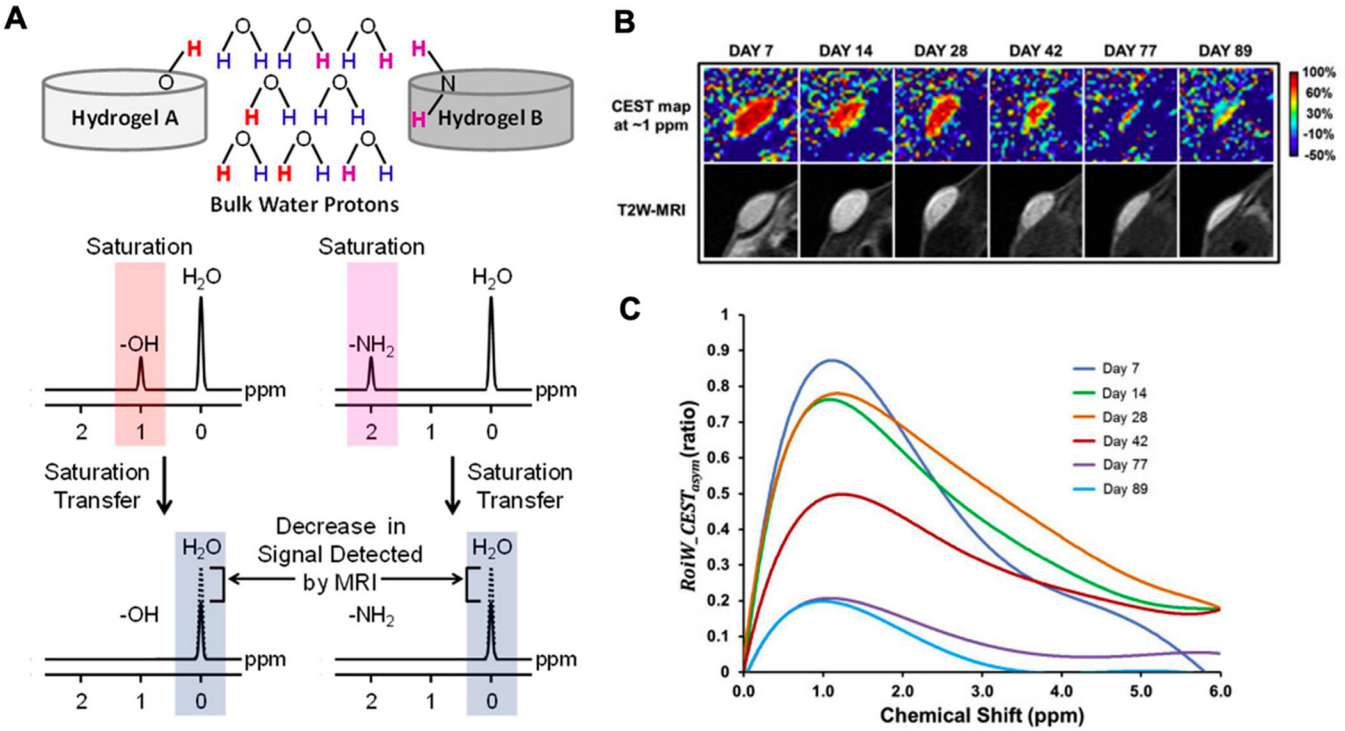

Figure 4.

(A) Principles of CEST for hydrogel imaging. Hydrogels can be differentiated based on their dominant exchangeable proton groups. (B) CEST maps and corresponding T_2-weighted MRI images from a dithiobis(ethylamine) (DTEA)-cross-linked HA hydrogel over time. (C) Quantification of CEST signal from the corresponding images over different time courses. Panel A is reproduced with permission from ref 119. Copyright 2015 American Chemical Society. Panels B and C are reproduced with permission from ref 53. Copyright 2018 Elsevier.

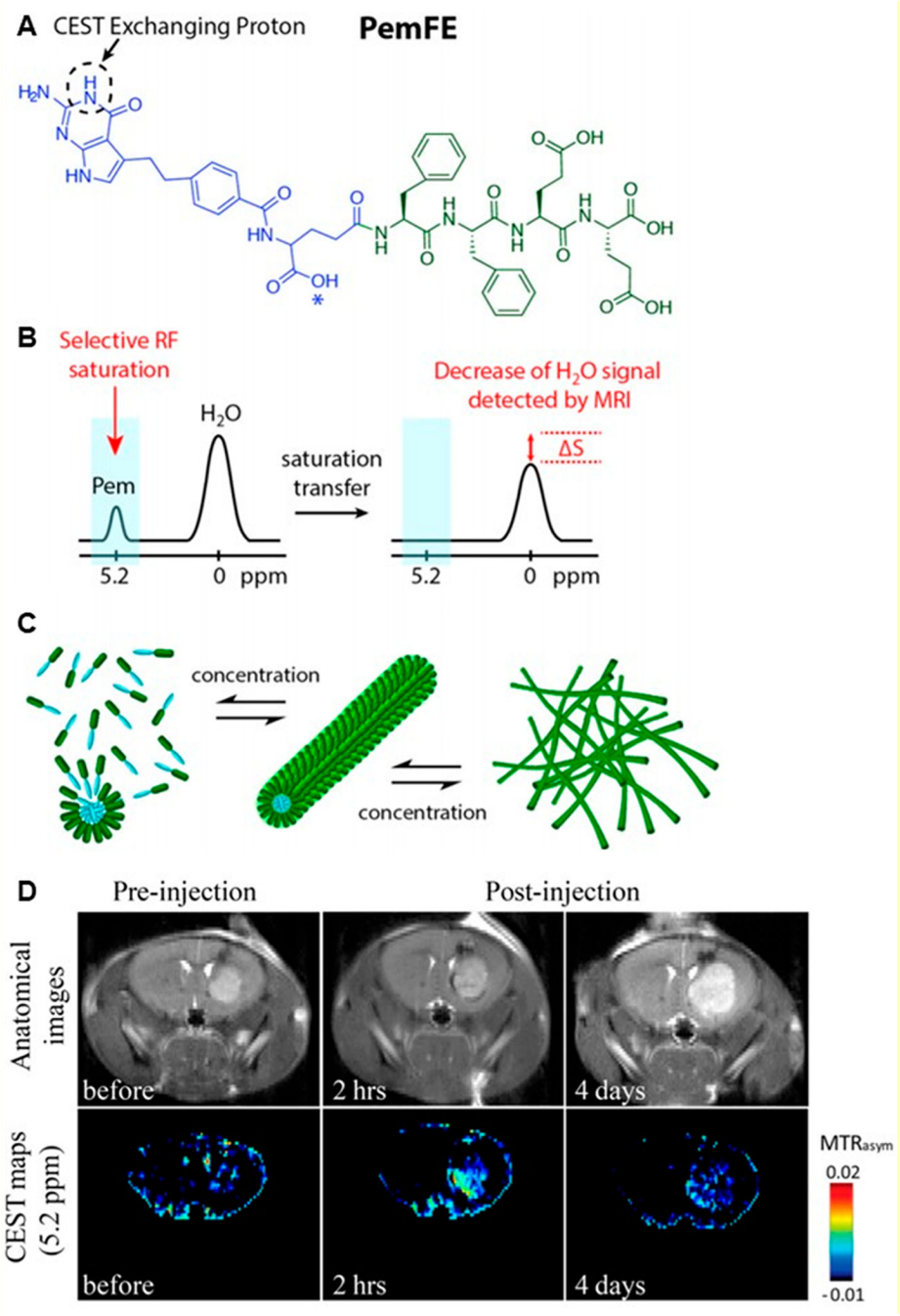

Figure 5.

(A) Structure of the pemetrexed-peptide conjugate, which (B) serves as a CEST probe with a chemical shift of 5.2 ppm and (C) self-assembles into a filamentous hydrogel as the concentration increases. (D) Monitoring the diffusion of the hydrogel by MRI (top) and CEST at 5.2 ppm (bottom) before and 2 h or 5 h postinjection in brain tumor. This figure is reproduced with permission from ref 118. Copyright 2017 American Chemical Society.

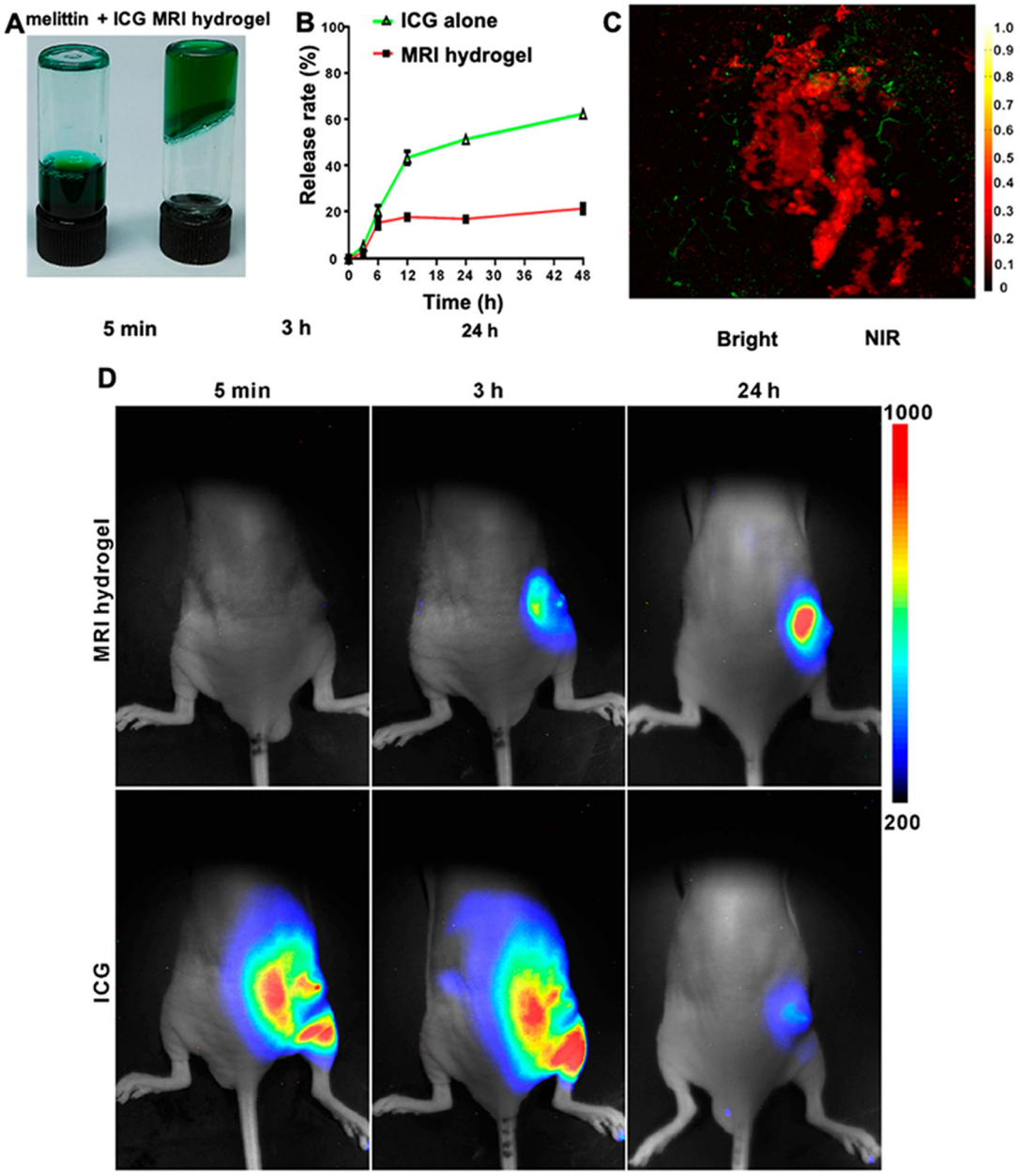

Figure 6.

(A) Photograph before (left) and after (right) gelation of the ICG loaded melittin-based hydrogel and (B) its ICG release profile. (C) Visualization by photoacoustic imaging of the ICG loaded melittin-based hydrogel (red) and solution of free ICG (green) after intratumoral injection. (D) NIR fluorescence monitoring of the biodistribution of the hydrogel (top) compared to free ICG solution (bottom) at various time points postinjection (5 min, 3 h, 24 h). This figure is reproduced with permission from ref 133. Copyright 2017 American Chemical Society.

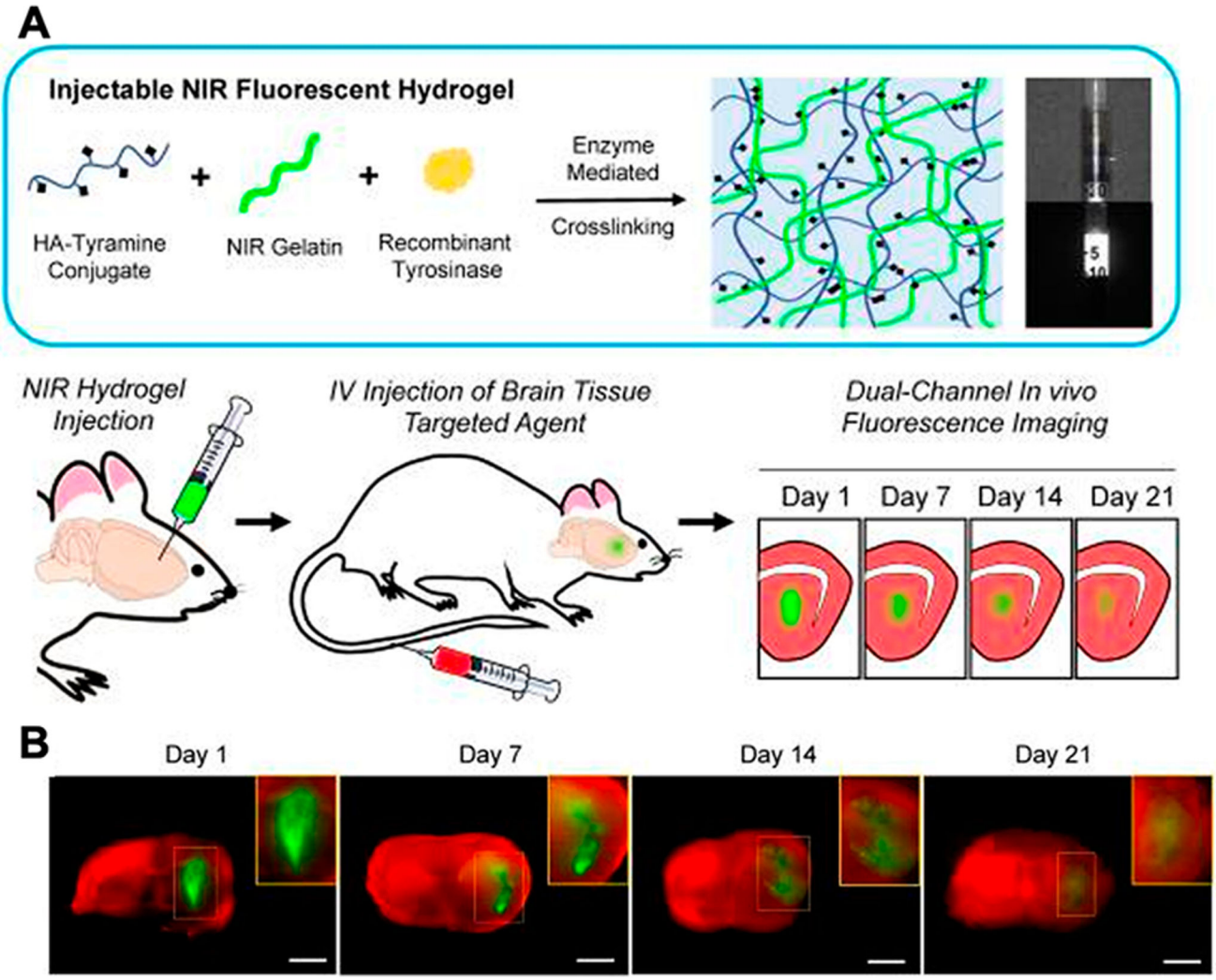

Figure 7.

(A) Schematic of the strategy of dual-channel fluorescence imaging for the *in vivo* assessment of brain tissue ingrowth and hydrogel scaffold degradation. (B) Fluorescent hydrogel and brain tissue targeted contrast agent Ox1 were administered to the animal. Dual-channel imaging was performed 1-h postinjection. Brain tissue ingrowth (red) and hydrogel (green) degradation can be observed in the merged image. This figure is reproduced with permission from ref 33. Copyright 2019 Ivyspring International Publisher.

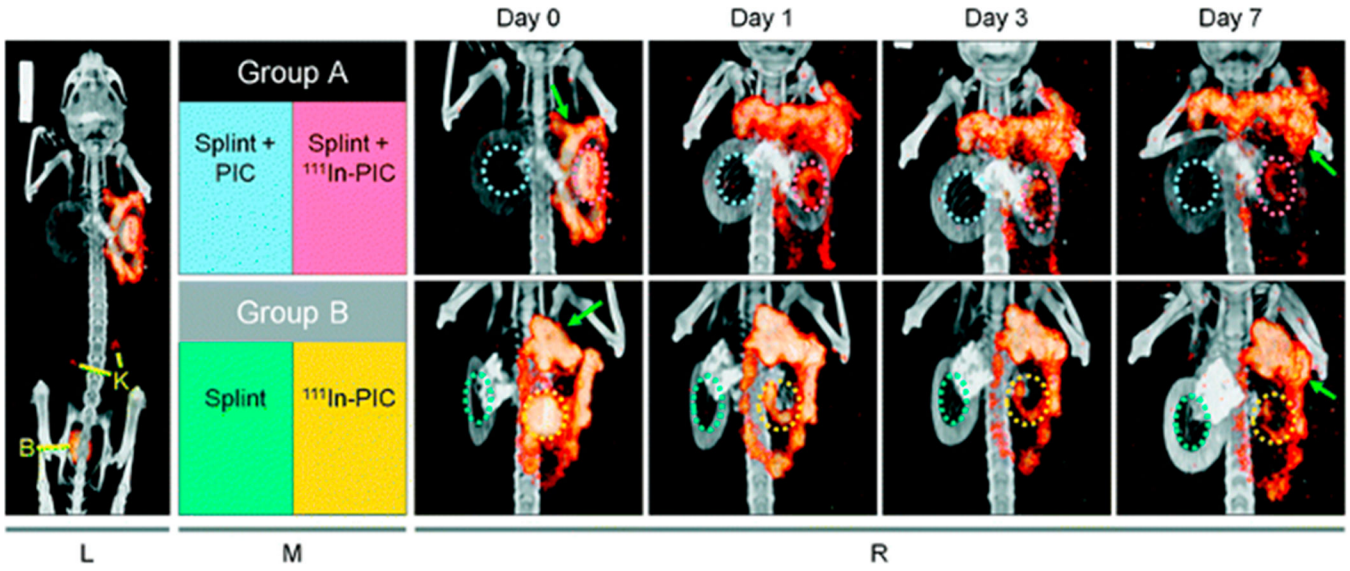

Figure 8.

Left panel (L): overview SPECT/CT scan of mice. SPECT signal from ^{111}In in the kidney and bladder is indicated with arrows. Middle panel (M): the different treatment conditions indicated by the dashed circles in the SPECT/CT scans to the right. Right panel (R): representative SPECT/CT images for mice under different treatment conditions. Green arrows indicate that the activities of hydrogels leaked away from the wound area but stayed close to the site of application. This figure is reproduced with permission from ref 145. Copyright 2013 Royal Society of Chemistry.

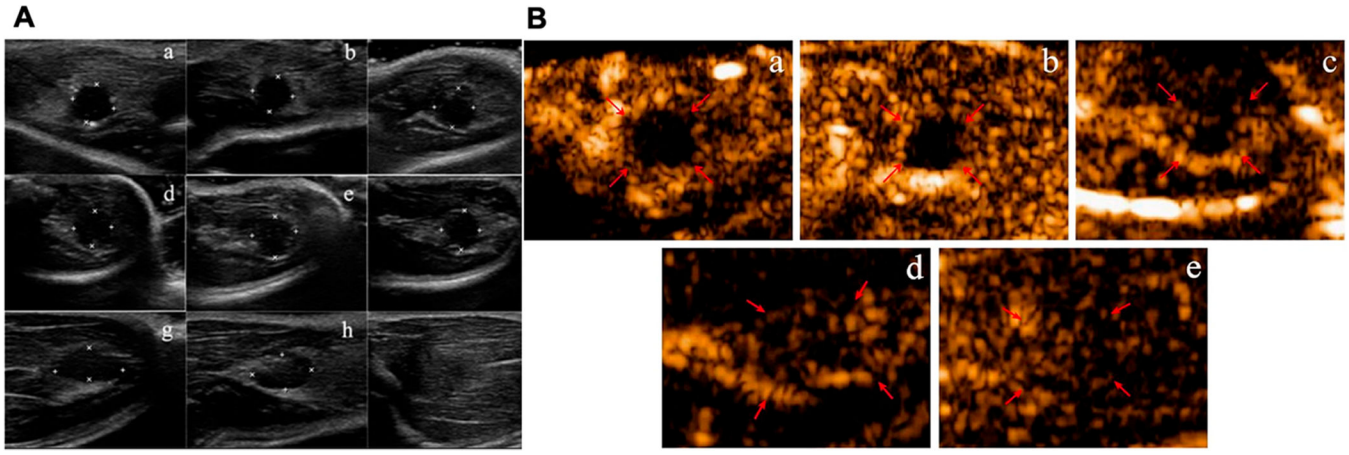

Figure 9.

(A) 2D greyscale ultrasound images of rat thigh with silk hydrogel implants. The echogenicity increased over time (a–f). (B) CEUS imaging of the hydrogel implants at different time points (a–e). More microbubbles infused into the gel matrix over time, indicating the progression of neovascularization. Red arrows indicate the outline of hydrogel implants. This figure is reproduced with permission from ref 34. Copyright 2015 John Wiley and Sons.

Table 1.

Characteristics of Imaging Modalities Used for Hydrogel Imaging[a]

imaging modality	advantages	limitations	source	contrast agents	common applications
CT	• high spatial resolution • anatomic imaging • low cost	• radiation • poor soft tissue contrast • common artifacts	X-rays	iodinated small molecules (A), barium sulfate suspension (A), gold nanoparticles	trauma, joints, cardiovascular diseases, gastrointestinal tract
MRI	• high spatial resolution • soft tissue contrast	• high cost • low sensitivity • long scan times	magnetic fields, radiowaves	gadolinium chelates (A), iron oxide nanoparticles, exchangeable protons	brain and spinal cord, musculoskeletal imaging, prostate and breast cancer imaging
nuclear imaging	• high sensitivity • quantitative • metabolic activity	• high cost • high radiation exposure	gamma-rays	radioisotopes (e.g., ^{18}F, ^{124}I) (A)	tumor imaging and cancer stage evaluation
optical imaging	• high sensitivity • multichannel imaging	• complex relationship between signal and probe concentration • poor tissue penetration	near-infrared (NIR) light	quantum dots, indocyanine green (A), methylene blue (A)	endoscopic and retinal imaging
photoacoustic	• noninvasive • high penetration depth	• not available in the clinic • limited field of view	nonionizing laser pulse/acoustic waves	quantum dots, gold nanoparticles, semiconducting polymers	hemodynamics monitoring
ultrasound	• widely available • low cost • portability	• common artifacts • low resolution • operator dependent	high-frequency acoustic waves	microbubbles (A)	fetus imaging, soft tissue imaging

[a]Note that while the poor soft tissue contrast of CT is typically viewed as a disadvantage for imaging, in the context of hydrogel imaging it may be an advantage, since it allows the hydrogel to be clearly distinguished from background soft tissue. On the other hand, the excellent soft tissue contrast of MRI can render identification of the hydrogel challenging due to a confounding endogenous signal. Note: The contrast agents have been FDA-approved for clinical use are noted with (A).

Table 2.

Overview of Multimodal Imaging Techniques and Their Common Applications

imaging modalities	applications	advantages
PET/CT	• tumor detection, cancer staging, and tumor response monitoring • assessment of targeted therapies	• clarification of equivocal CT findings • improved spatial resolution and lesion characterization
SPECT/CT	• musculoskeletal infection, trauma, and malignant disease imaging • cardiac imaging	• increased specificity through more precise localization and characterization
PET/MRI	• tumor staging and presurgical planning for oncological conditions associated with soft tissues	• reduced ionizing radiation • provides simultaneous anatomic and molecular information
ultrasound/CT	• soft tissue imaging • breast cancer diagnosis	• produces quantitative images of the acoustic properties of tissue

ACS Biomater Sci Eng. Author manuscript; available in PMC 2022 September 13.

Table 3.

Representative Hydrogel Formulations and Modifications for Imaging[a]

imaging modality	imaging functionalization	polymer	cross-linking method	refs
		Intrinsically Imageable Hydrogels		
CEST MRI	N/A	alginate/liposomes	ionic cross-linking (Ca^{2+})	Han et al. (2020)[117]
CEST MRI	N/A	HA-SH/gelatin-SH	Michael addition (PEG-diacrylate)	Zhu et al. (2019)[52]
CEST MRI	N/A	peptide conjugate (glutamic acid + phenylalanine)	amphiphilic peptide self-assembly	Lock et al. (2017)[118]
CEST MRI	N/A	HA	Michael addition (divinyl sulfone)	Shazeeb et al. (2018)[53]
CEST MRI	N/A	hydroxyethyl methacrylate-modified HA (HeMA-HA)	radical polymerization	Dorsey et al. (2015)[119]
fluorescence	N/A	polyacrylamide	radical polymerization	Xu et al. (2019)[120]
fluorescence	N/A	multiarm PEG acrylates	Michael addition	Tsou et al. (2018)[121]
fluorescence	N/A	bovine serum albumin (BSA)/ human serum albumin (HAS)	enzymatic (glutaraldehyde)	Ma et al. (2016)[122]
		Physical Loading of Contrast Agents		
CT	gold nanoparticles	gelatin-tyramine	enzymatic	Lee et al. (2018)[110]
CT	gold nanoparticles	PNAGA-PAAm copolymer N-acryloyl glycinamide	radical polymerization	Wu et al. (2018)[123]
CT	gold nanoparticles	alginate	ionic cross-linking	Keshavarz et al. (2018)[124]
CT	gold nanoparticles	gelatin methacrylamide (GelMA)	radical polymerization	Celikkin et al. (2019)[125]
CT	iopidamol and tantalum oxide particles	gelatin-tetrazine/gelatin-norbornene	dynamic covalent (Diels–Alder)	Hong et al. (2016)[31]
CT	platinum nanoparticles	alginate	ionic cross-linking	Wang et al. (2016)[126]
CT	barium sulfate suspensions	polyacrylonitrile (PAN)	radical polymerization hydrogen bonding	Zhang et al. (2018)[127]
fluoroscopy	iodinated contrast agents	chitosan	ionic cross-linking	Coutu et al. (2012)[128]
MRI	M-ferrite nanoparticles	AMPEG550	hydrophobic association	Kim et al. (2012)[129]
MRI	DTPA-Gd (III)	chitosan-DTPA	Schiff base (PEG-dialdehyde)	Liu et al. (2016)[32]
MRI	DOTA-Gd(III)	polyethylene glycol (PEG)	hydrogen bonding	Bakker et al. (2018)[48]
MRI	ferumoxytol	chitosan	hydrogen bonding	Chen et al. (2020)[130]
MRI	iron oxide nanoparticles	dehydrodipeptides	peptide self-assembly	Carvalho et al. (2019)[131]
fluorescence	carbon nanodots	N-methacryloyl chitosan	radical polymerization	Wang et al. (2017)[132]

imaging modality	imaging functionalization	polymer	cross-linking method	refs
fluorescence	indocyanine green (ICG)	RADA16-I peptide	peptide self-assembly	Jin et al. (2017)[133]
fluorescence	CdTe and CdSe quantum dots	Fmoc-diphenylalanine	peptide self-assembly	Kim et al. (2010)[134]
fluorescence	$NaYF_4$:Yb,Er@PAA upconversion nanoparticles	GelMA	radical polymerization	Dong et al. (2017)[61]
fluorescence	$NaLuF_4$:Er^{3+}, Yb^{3+} @graphene oxide (NGO) nanoparticles	gelatin	hydrogen bonding	Li et al. (2019)[135]
fluorescence	$NaLuF_4$:Er^{3+}, Yb^{3+} @graphene oxide (NGO) nanoparticles	silk fibrin	peptide self-assembly	He et al. (2018)[136]
photoacoustic	ferrous/ferricyanide ions	dibenzaldehyde-terminated telechelic PEG (DF-PEG)/chitosan	dynamic covalent (Schiff base)	Cheng et al. (2017)[137]
ultrasound	SonoVue microbubbles	silk fibrin	peptide self-assembly	Leng et al. (2015)[34]
fluorescence/ photoacoustic	Ag_2S quantum dots	polypeptide PC_{10}	peptide self-assembly	Jin et al. (2019)[36]
MRI/fluorescence/ ultrasound	Zn ferrite magnetic nanoparticles (MNPs) and ICG	PEG diacrylate (PEG-DA)	radical polymerization	Wu et al. (2017)[138]
		Chemical Grafting of Contrast Agents		
CT	2,3,5-triiodobenzaldehyde	polyvinyl alcohol (PVA)	radical polymerization	Ashrafi et al. (2017)[15]
MRI	F19	HA-carbazate	Michael addition	Yang et al. (2014)[105]
MRI	gadolinium complex	HA-aldehydeHA-hydrazide	dynamic covalent (Schiff base)	Bermejo-Velasco et al. (2018)[139]
MRI	GdDOTA nanoparticles	chitosan/HA	ionic cross-linking	Courant et al. (2012)[140]
MRI	iron oxide nanoparticles	cellulose nanocrystal/silk fibroin	peptide self-assembly	Chen et al. (2018)[16]
fluorescence	near IR-gelatin	HA-tyramine gelatin	Enzymatic (tyraminadase)	Park et al. (2019)[33]
fluorescence	bodipy-aldehyde	chitosan	dynamic covalent (Schiff base)	Belali et al. (2017)[62]
fluorescence	glucose-responsive fluorescent monomer	PEG-bonded polyacrylamide (PAM)	radical polymerization	Heo et al. (2011)[141]
fluorescence	protoporphyrin	PCL-PEG-PPOR-PEG-PCL	hydrophobic associations	Dong et al. (2016)[142]
SPECT/CT	$Ba^{2+}In^{3+}Zr^{4+}$	alginate	ionic cross-linking	Patrick et al. (2020)[63]
SPECT/CT	DOTA-In^{3+}	amphipathic hexapeptide H-FEFQFKNH2	amphipathic peptide (β sheet)	Oyen et al. (2017)[143]
SPECT/CT	^{99m}Tc	carboxymethyl-cellulose	hydrogen bonding	Lauren et al. (2014)[144]
SPECT/CT	indium-111 (^{111}In)	polyisocyanopeptide (PIC)	peptide self-assembly	Op't Veld et al. (2019)[145]
scintigraphy	^{131}-I	chitosan	ionic cross-linking (TPP)	Kim et al. (2014)[35]
fluorescence/MRI/ ultrasound	rhodamine B and $CoFe_2O_4$ nanoparticles	PLGA-PEG-PLGA	amphiphilic block copolymers	Chen et al. (2020)[146]

[a] N/A: not available.

ACS Biomater Sci Eng. Author manuscript; available in PMC 2022 September 13.